AMC

Thin-Wall and High-Strength Die Casting Alloys

Final Report

D. Schwam

Case Western Reserve University

Allan Miller

Ohio State University

September 2017

Abstract

NADCA has had success in developing a zinc alloy chemistry and processing parameters for thin-wall zinc applications. This project envisioned development of the same methodology to aluminum in order to produce thinner wall castings for light weighting. In addition, since higher fluidity is required for thin-wall casting, this project enables complex geometries to be made that cannot otherwise be successfully produced and allows scrap issues stemming from lack of fill to be reduced or eliminated.

Working with NADCA, the project team attempted to develop alloy composition(s) with high fluidity in aluminum by:

- Defining composition for a high-fluidity aluminum die casting alloy
- Measuring and optimizing fluidity of potential Al alloys
- Casting test bars to measure mechanical properties

An initial effort was dedicated to developing an instrument capable of measuring fluidity of aluminum alloys under conditions similar to die casting. This instrument was comprised of a vacuum reservoir connected to a vent block. The vent block was in turn connected to a silicon carbide riser tube immersed in molten aluminum. By applying vacuum to this system, molten aluminum is sucked into the vent block. The distance traveled by the molten alloy before it solidifies is used as a measurement of fluidity. Using this instrument, a range of commercial aluminum alloys were evaluated. The high silicon 390 aluminum alloy had the highest fluidity. Increases in the silicon and copper in this alloy provided even higher fluidity, although the increase was very modest. In laboratory trials, boron nitride coatings applied on the vent block were also shown to improve fluidity. Preliminary in-plant trials were also conducted with a boron nitride coating. Additionally, the mechanical properties of alloys evaluated in this study were measured using test bars die cast at Premier Die Casting and are detailed in this report.

Parallel to the experimental work, a computational effort to predict influences of processing variables on fluidity was undertaken by Ohio State University. This work is described in a separate report. A relatively simple one-dimensional heat transfer model that incorporates part wall thickness, injection and die temperatures, gate speed plus the freezing range and fraction solid curve of the alloy was developed. The basic fluidity model was extended to incorporate varying speed and/or wall thickness. This extension enables analysis of prefill, or the situation where the cavity is partially filled before the onset of the fast shot or high-speed phase of cavity filling, and provides insight into the conditions under which prefill is beneficial and where it is not likely to be successful.

Several computation factorial experiments were performed using the basic model and analyzed to understand the relative importance of each factor as a contributor to flow distance. The results show that, while the alloy properties do affect the flow distance,

flow distance or fluidity is largely a thermal issue controlled by the process conditions. This result provides support for the observation that the casting alloy should be selected to meet the functional requirements of the part without undue consideration of fluidity. The process conditions can then be optimized to produce an acceptable casting.

The computational work showed the injection velocity to be by far the most important variable in improving filling. The interfacial heat transfer between the die and the solidifying metal was also shown to have a significant impact on flow distance. This is an important takeaway, since it could be used by die casters to facilitate casting of thin-wall parts.

A subtask of the project addressed semi-solid metalcasting (SSM) casting of high-strength aluminum alloys. Standard high-pressure die casting (HPDC) of high-strength aluminum alloys such as 201 and 206 that are typically used in gravity pour methods is difficult due to the extremely low silicon content of these alloys. Because the flow and fill characteristics of semi-solid slurries are different than HPCD and because hot tearing is reduced due to lower pour temperatures, it was thought that it might be possible to cast these types of alloys in highly complex configurations by the semi-solid process. Although such alloys have been SSM cast, processing parameters that provide a wide operating window have not been established. This project evaluated SSM parameters designated for robust processing of high-strength alloys and demonstrated the process by casting test plates. Alternative compositions of aluminum 201 and 206 alloys for squeeze processing were identified from literature and mechanical properties were reported.

Partner companies such as General Die Casters, TCDC, Eck Industries, Mercury Marine and others have been steadily pushing the limits of thin wall die castings by introducing vacuum technology and optimizing the process parameters. Provided rigorous controls are in place, wall thickness sections of less than 1mm can be produced. The combined experimental and computational efforts put forth in this project are making a modest contribution to this industry-wide effort. They demonstrate slight variations in fluidity to have a lesser impact on filling of thin wall die castings than process and thermal variables, such as shot velocity and heat transfer.

TABLE OF CONTENTS

1. Driving Force for Thin-Wall Castings

Dynacast articulated well the driving force for thin-wall casting on their website https://www.dynacast.com/blog-thin-wall-cast-aluminum. “What if I told you that we can now cast aluminum parts that are almost as lightweight as their magnesium counterparts and offer more benefits like higher tensile strength and additional finishing options?” In the past, design engineers have shied away from aluminum die casting because of the need for thicker wall sections (typically 1.5mm – 2.0mm) and the resultant heavier parts.

You might be asking yourself, “Why is it difficult to cast aluminum with thin walls?” Well, aluminum has a very high melting and freezing point so when molten metal is injected into a die, the aluminum starts cooling quickly and becomes solid. The window between the liquid state and the solid state is very narrow, which means the fill time needs to be less than 30 milliseconds for a thin-wall (0.5mm – 1.0mm) feature to be created. Die casting engineers can do this with extremely precise process control—even small adjustments to more than a dozen variables can be the difference between success and failure. Good tooling design is equally important. Tooling engineers need to find the perfect balance of the runner system and gating design, proper overflow placement and design, and targeted thermal management.

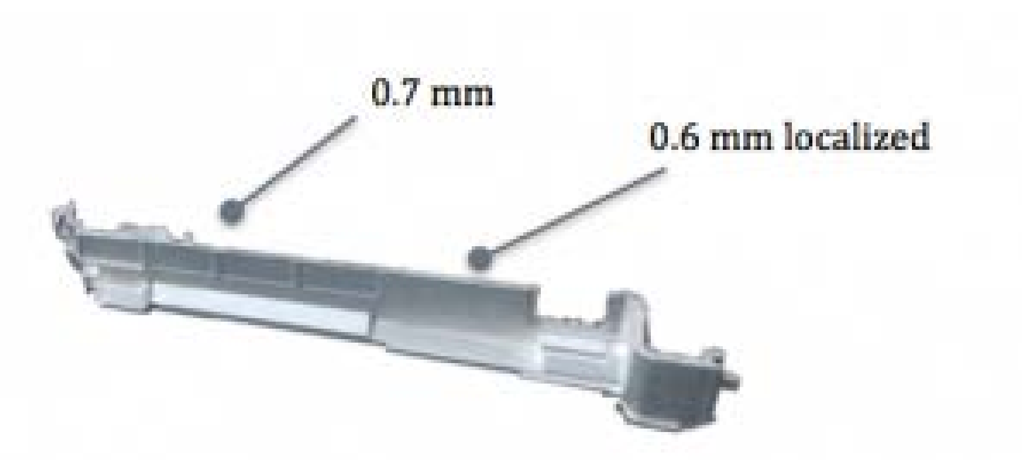

Figure 1.1: Example of a thin-wall casting

Evolution of Thin-Walled Aluminum Technology

Historically, in order to cast aluminum with thin-wall sections, custom-formulated high-fluidity alloys would have been used. However, recently developed methods can be applied to die cast thin wall castings using standard alloys by <u>using improved process control, state-of-the-art tool design, and machine enhancements.</u>

Benefits of Thin-Walled Aluminum Die Casting

One of the most important benefits of thin-walled aluminum die casting is that it creates lighter parts—with more surface finishing options than other die cast alloys. Creating a part with 0.5mm walls instead of 2mm offers a 75% reduction in weight, which is a big deal—especially when you're trying to take weight out of an automobile component or a hand-held mobile device. Aluminum can also withstand the highest operating temperatures of all the die cast alloys. Moreover, cast aluminum is versatile and corrosion resistant; it retains high dimensional stability with thin walls, and can be used in almost any industry.

2. Project Objectives

The general sense in the die casting industry is thinner sections pose filling deficiencies and high-strength alloys are by and large not die-castable. Light-weighting of parts with thinner sections requires improvements in filling by improved fluidity or slower heat transfer during filling. The original objectives of the project were to improve fluidity of alloys, processing parameters, and die-design methods for thin-wall applications. A complementary goal was to identify and employ insulating die lubricants or coatings to improve die filling. Developing SSM and squeeze casting process parameters for high-strength alloys such as A201 and A206 were the goals of the SSM task of the project.

3. Literature Survey

3.1 Thin-Wall Castings

Advances in thin-wall die casting are rather segmented and described in the technical literature under a variety of technologies. The bulk of the information is included in vacuum die casting, computer simulation, processing, die lubricants, die design and alloy development. Indeed, successful production of thin-wall die castings involves fine tuning multiple aspects of die casting design and processing. It frequently requires pushing the die casting process to its limits.

One of the early adopters of vacuum die casting was Contech (now Shiloh), who has been practicing vacuum assist since the early 80's and licensed high-vacuum High-Q-Cast since 2004. This high-integrity die casting process is capable of producing large, thin-wall (2mm-4mm) structural castings. Such large thin-wall castings can be used to replace steel stampings in the car body and chassis (i.e. shock towers, pillars, door frames, etc.). A car body represents approximately one quarter of the vehicle weight and offers the greatest potential for weight savings. Aluminum can save up to 50% of a car body structure weight compared to the equivalent steel structure and still match or exceed structural stiffness and crashworthiness requirements (Jorstad J.J.2008).

Figure 3.1.1: BMW X5 Front Shock Tower (Brown Z, 2008)

The BMW X5 Front Shock Tower (Emmenegger, 2006) illustrated in Figure 3.1.1 requires high elongation for crash performance. By employing the High-Q-Cast™ high vacuum process on a 2,500 ton machine with Aural-2 (AlSi10MgMn) and a T6 heat treat, high mechanical properties were obtained (YS=120-140 MPa, TS=180-200 MPa, El=12-16%). Simulation was employed to design the gating, so the flow and solidification pattern were adequate. Another part cast by the High-Q-Cast™ high vacuum process is the B-pillar illustrated in Figure 3.1.2. It is 48 inches long and weighs 4.4 pounds.

Figure 3.1.2: B-Pillar cast by the High-Q-Cast™ high vacuum process

The high vacuum assists with filling of thin sections and the complete filling of remote and isolated regions in die cavities by reducing or eliminating the resistance of trapped air to the flow. It also promotes low porosity, since the main source of porosity in die cast components are gases entrapped during turbulent cavity fill. Control of the shot profile, good gating practices, adequate die temperatures and careful venting also serve to minimize gas entrapment. This in turn enables heat treating of the castings with no blistering. Achieving the level of vacuum needed to render a die casting heat treatable without blistering, e.i.100 millibar (0.1 atmospheres) or less, requires several special considerations (Brown Z, 2006):

- Seals – High levels of vacuum may require that mating die surfaces be ground and that various types of seals be applied at all parting faces and around slides.
- Lubricants – Only certain water-borne lubricants are suitable, as the carrier must quickly evaporate leaving no residuals to volatilize during the shot.
- Gating – Depending on part size and wall thickness, gating of high-vacuum die castings must often be more generous than is the case for most conventional HPDC cases.
- Venting – Die cavity vents communicating with the vacuum may require tortuous paths to prevent molten metal from invading and plugging vacuum valves.

Sound parts with a wall thicknesses of 2mm or less can be made using High-Q-Cast. Parts are usually gated with 20-30 gates, in contrast to 3-4 gates in conventional die casting. Maintaining the correct die temperature is critical in die casting thin-wall castings. For this purpose, the cooling lines must be properly sized and placed, and the die temperature must be controlled to stay within a narrow band with thermocouples that adjust the water flow. Thin-wall castings require minimal removal of heat from the surface of the cavity, thus shorter spray times and use of high ratios of lube to water. This often translates into hotter cavity temperature, thus the lube formulation needs to be adjusted to prevent premature decomposition with potential release of gas.

In some cases, vacuum assist methods can be used as a lower cost alternative. However, vacuum assist will usually not be sufficient to die cast parts with the wall-thicknesses feasible with high vacuum. Table 3.1.1 highlights some of the technical differences between vacuum assist and high-vacuum die castings (Robins, P, 2003).

Table 3.1.1: Technical differences between vacuum assist and high-vacuum die

Feature	HPDC (vacuum assist)	High-Q-Cast[R]
Degassed metal	Lesser degree	Higher degree (>97% density index preferred)
Metal transfer into cold chamber	Ladle	Dosing furnace
Preferred wall thickness	3 - 8 mm	2 – 5 mm
Sealed dies	No	Yes
Vacuum level	24 – 28” Hg	>29” Hg
Vacuum valve type	eg. Thurner	Optimized vacuum valve
Vacuum valve close	Before fast shot	During fast shot
Advanced vacuum monitoring	No	Yes
Cavity humidity measurement	No	Yes
Importance of die spray and tip lube selection	Low	Very high
Solution treatable	No	Yes
Weldability	No	Yes
Commonly used alloys	380, 383	Aural – 2 and 3
Mechanical properties	Moderate strength and low ductility	High strength and/or high ductility
Susceptibility to shrink porosity/oxide	High	Low

Meridian has been a leader in thin-wall aluminum and magnesium die castings. A typical example is the Mg Viper dashboard shown in Figure 3.1.3.

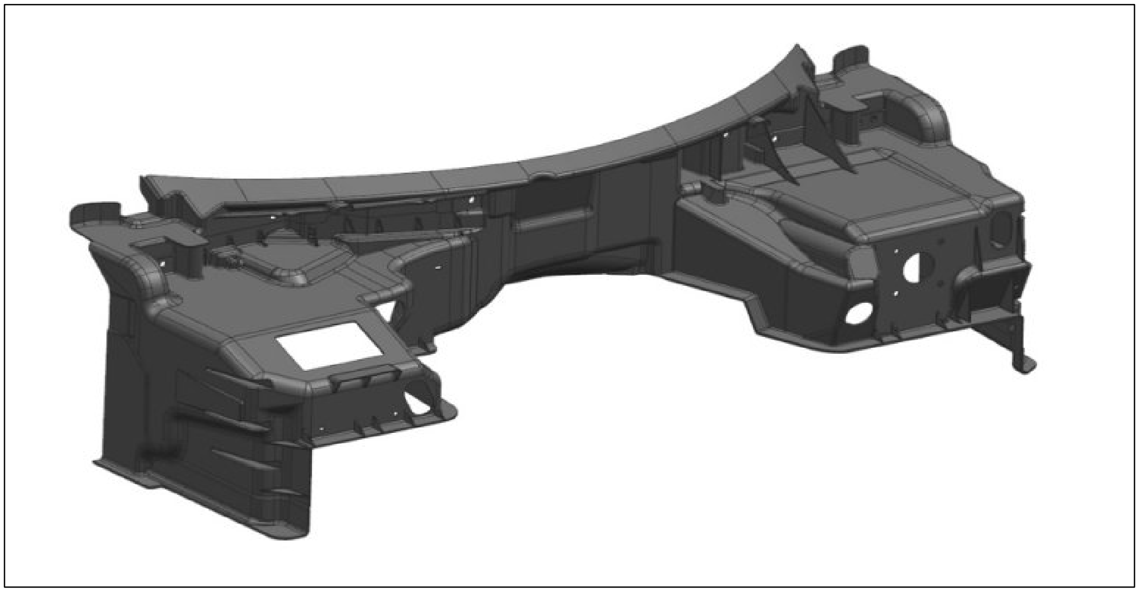

Figure 3.1.3: Die Cast Mg Viper Dashboard

A few other examples are shown in the following Figures 3.1.4-3.1.8.

Figure 3.1.4: DeimlerChrysler Class C and Class S Engine Cradles

Die caster: Honsel, Germany

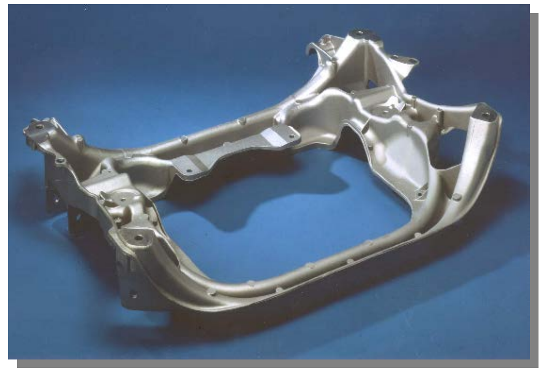

Alloy: GD-AlSi9MgMn T2 (Special alloy, vacuum) Dimension:	Alloy: GD-AlSi9MgMn T7 (Special alloy, vacuum) Dimension:

Figure 3.1.5: BMW Automotive Dashboards

Method: Castool Vacuum

(Robins)

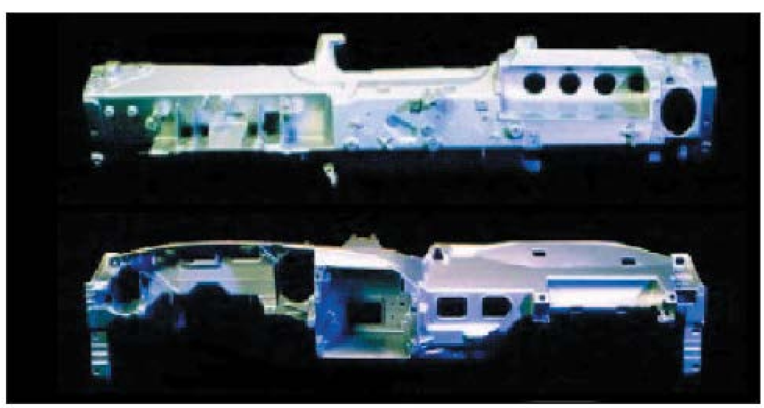

Figure 3.1.6: Automotive Dashboard

Method: Fondarex

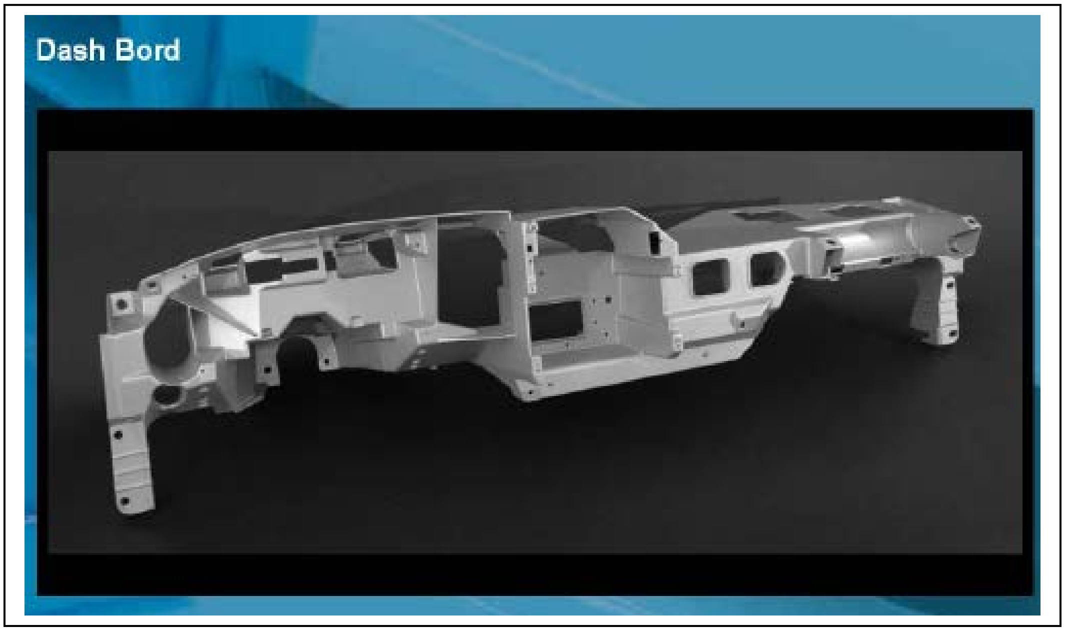

Figure 3.1.7: Automotive Suspension

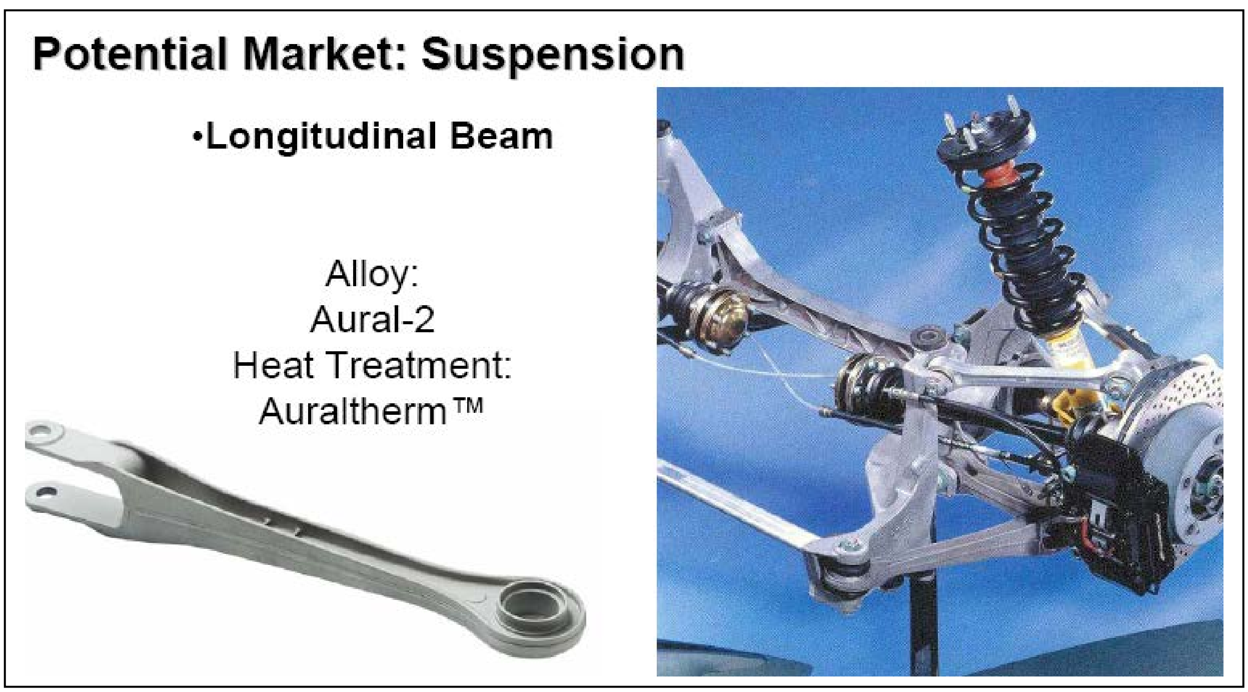

Figure 3.1.8: Automotive Door Components

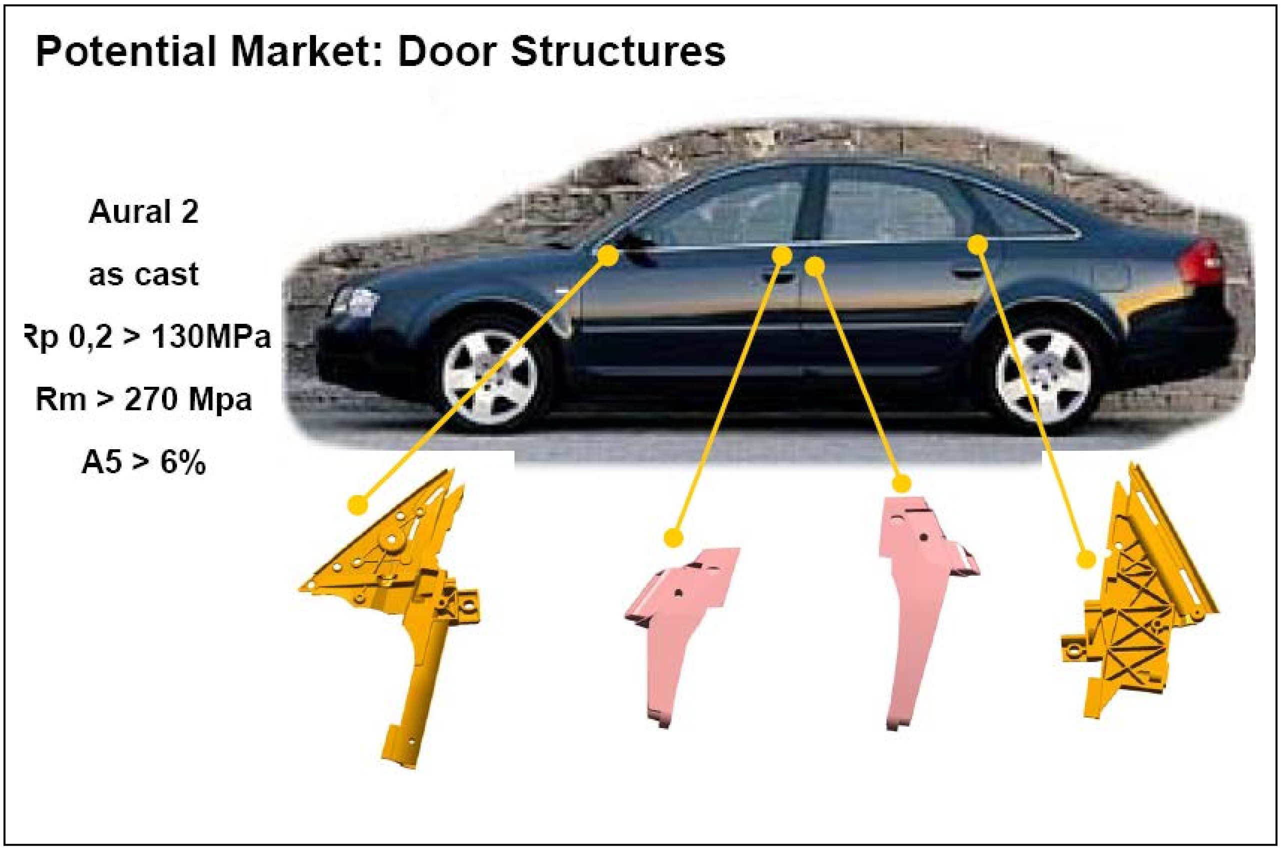

3.2 Fluidity of Aluminum Alloys

Fluidity of molten metals is of much practical importance for metal casters as it affects the ability of the metal to fill the mold. Unlike fluidity that is a characteristic of the liquid metal alone, fluidity also depends on the mold. As such, it is a more complex variable. Fluidity of molten aluminum alloys has been studied mainly in the context of sand and permanent mold castings. Most studies have used a spiral configuration to measure fluidity. In a recent study, (Pucher et. al. 2010) used the testing configuration shown in Figure 3.2.1. They define fluidity as the maximum distance L_f, to which the metal fills the spiral mold, i.e. the length of the molten alloy can flow until it is stopped by solidification.

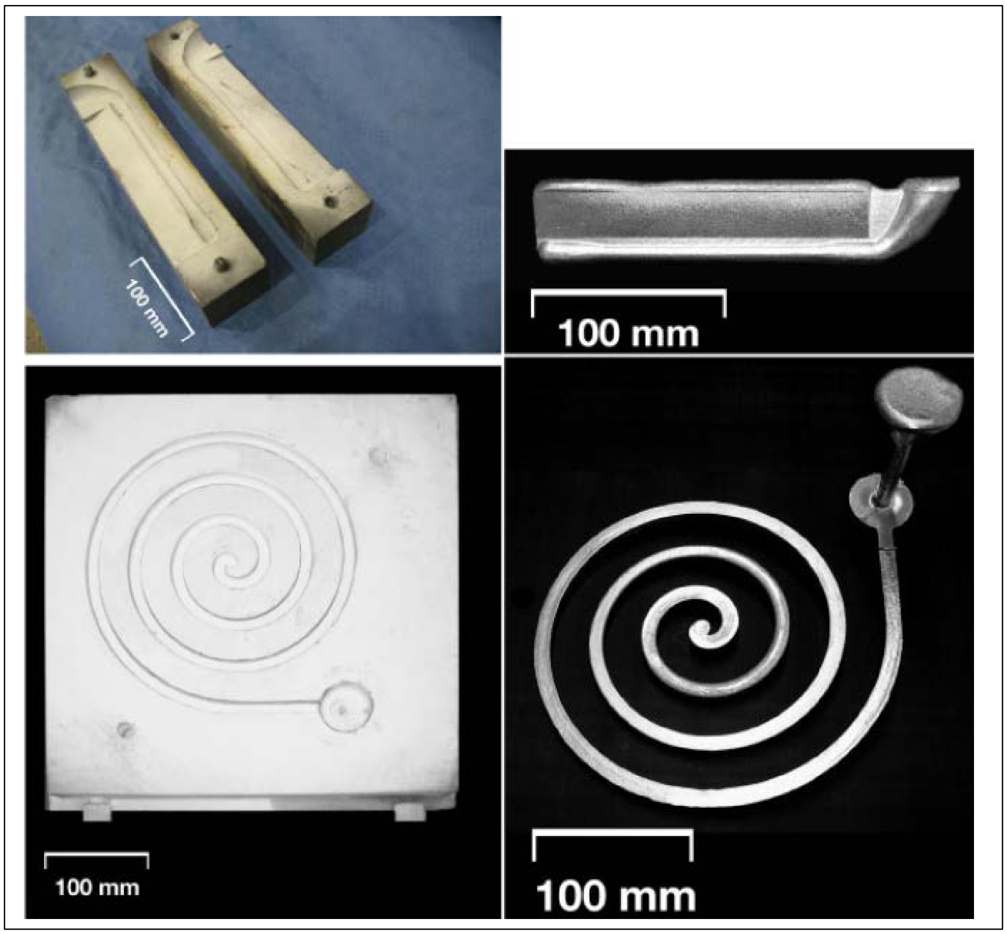

Figure 3.2.1: Typical spiral mold configuration used in fluidity studies of casting alloys

Among other findings, the Pucher study concludes higher silicon increases fluidity over a wide range of temperatures as illustrated in Figure 3.2.2.

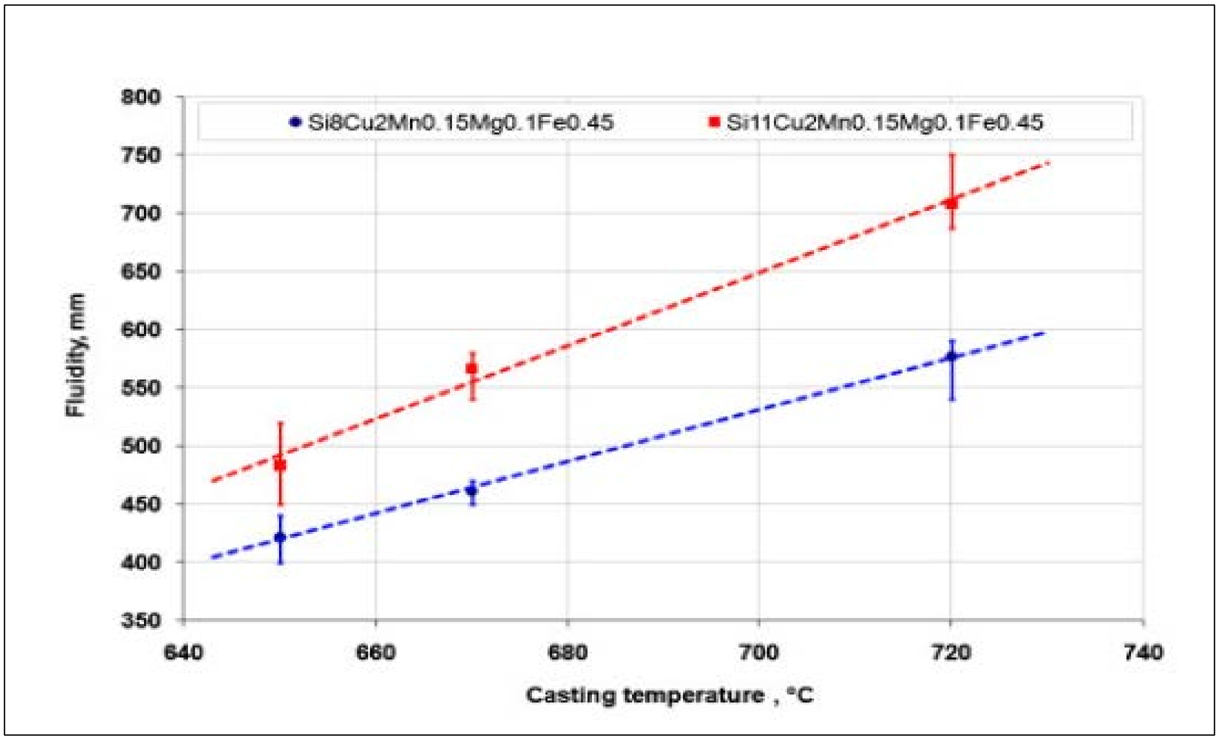

Figure 3.2.2: Casting temperature v. fluidity: alloys with high Si content exhibit higher fluidity

In a comprehensive review on fluidity of aluminum foundry alloys, (Di Sabatino, 2005) discusses the marked effect of silicon on fluidity in binary alloys, as shown in Figure 3.2.3. A peak in fluidity appears around 17-18% silicon. Indeed, 390 aluminum alloy with this silicon content is among the highest fluidity alloys, as illustrated in Figure 3.2.4 that shows the relative fluidity of commercial foundry aluminum alloys. Note the further improvement in fluidity for the 17% Si alloy.

The effect of copper on the fluidity of binary aluminum alloys is shown in Figure 3.2.5. The fluidity decreases initially up to 10% copper then start increasing up to the eutectic composition of 33% copper.Magnesium additions also cause an initial decrease in fluidity followed by an increase up to about 38% Mg as shown in Figure 3.2.6.

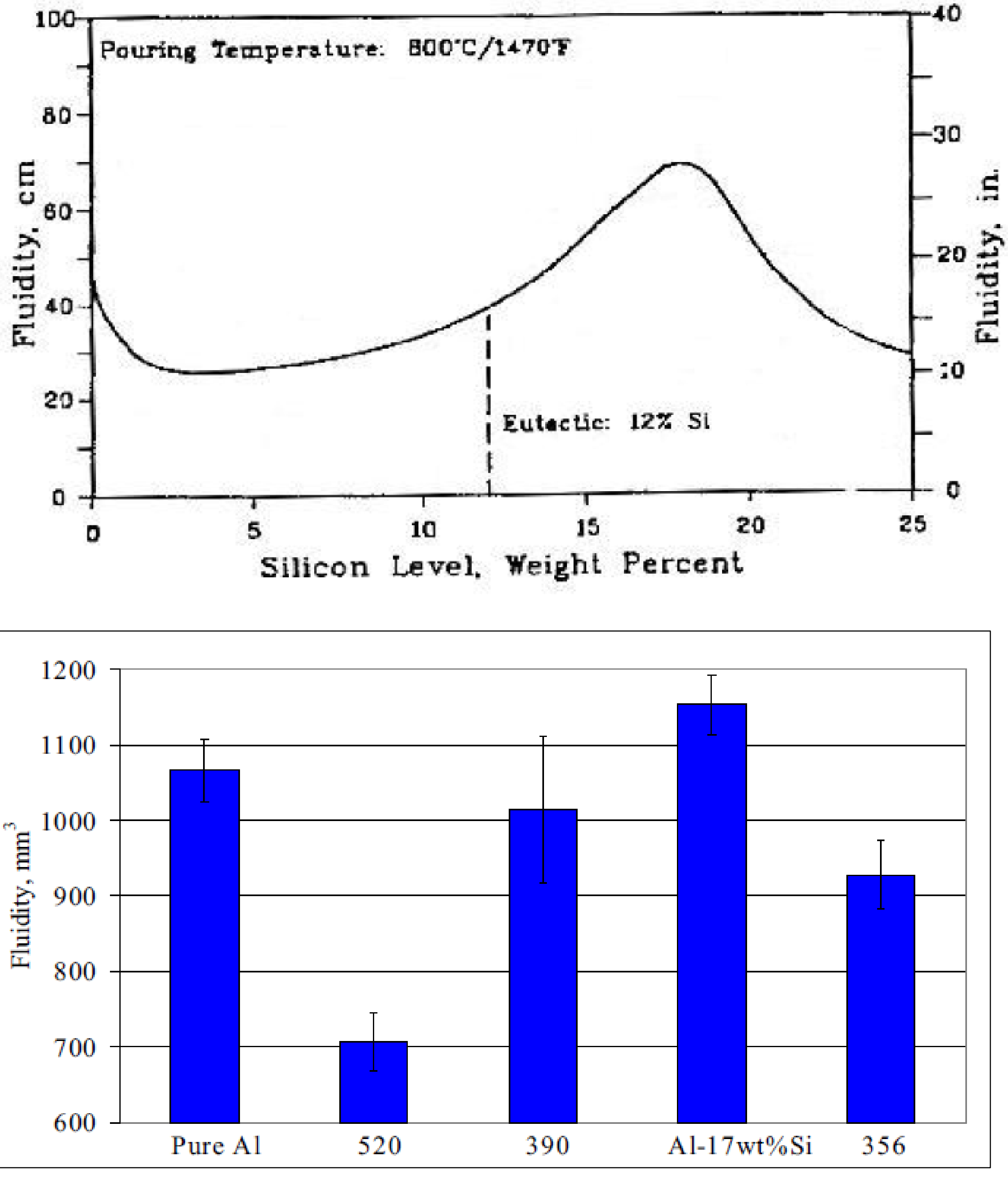

Figure 3.2.4: Relative fluidity of commercial foundry aluminum alloys

DISTRIBUTION STATEMENT A. Approved for public release: distribution unlimited

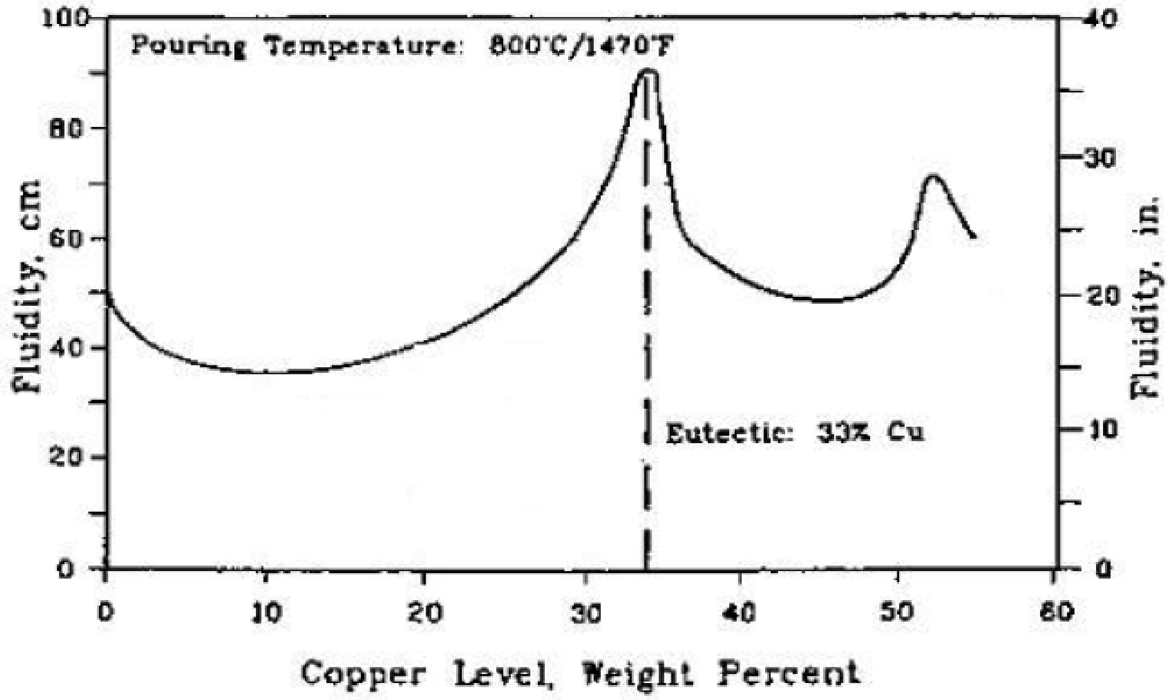

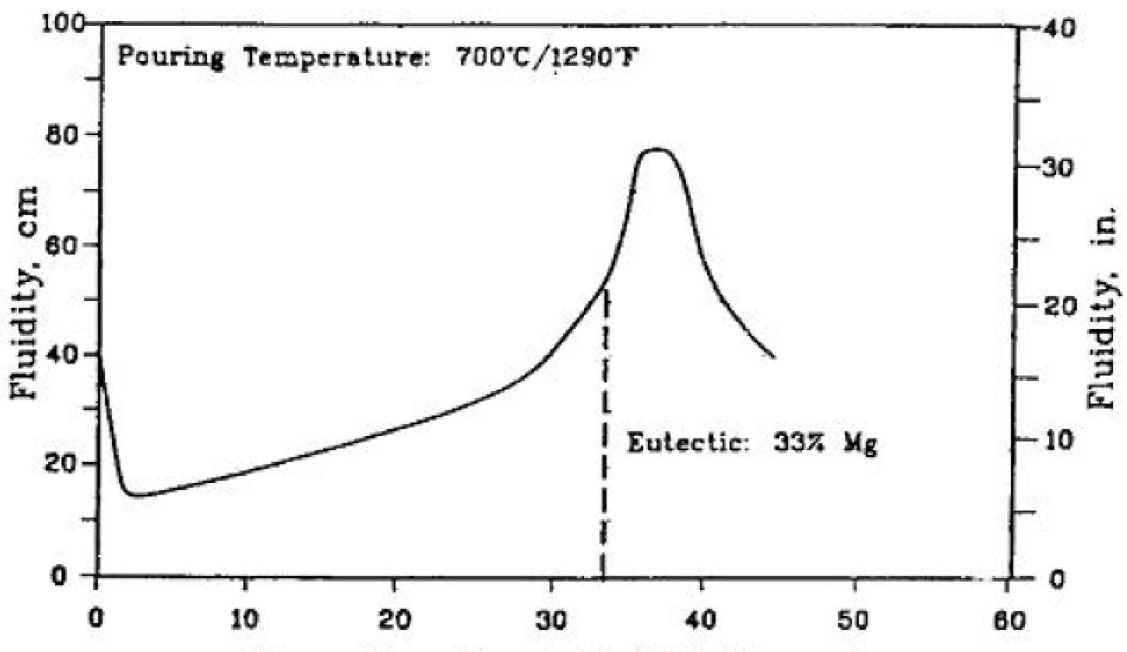

Figure 3.2.6: Effect of magnesium on fluidity in aluminum binary alloys

4. Development of an Experimental Method for Measuring Fluidity

The suitability of fluidity measurement methods used in the metal casting industry was assessed early in the project. Since fluidity depends not only on the molten metal but also on the characteristics of the mold, the general feeling was a customized set-up was desirable. Rather than a sand mold and gravity pour, this set-up should include a metal mold, as well as high-velocity filling. The ultimate method is to use a die casting machine. However, a simpler set-up that is compatible with a well-controlled laboratory evaluation and can generate quantitative data seemed adequate. The schematic set-up illustrated in Figure 4.1 was suggested.

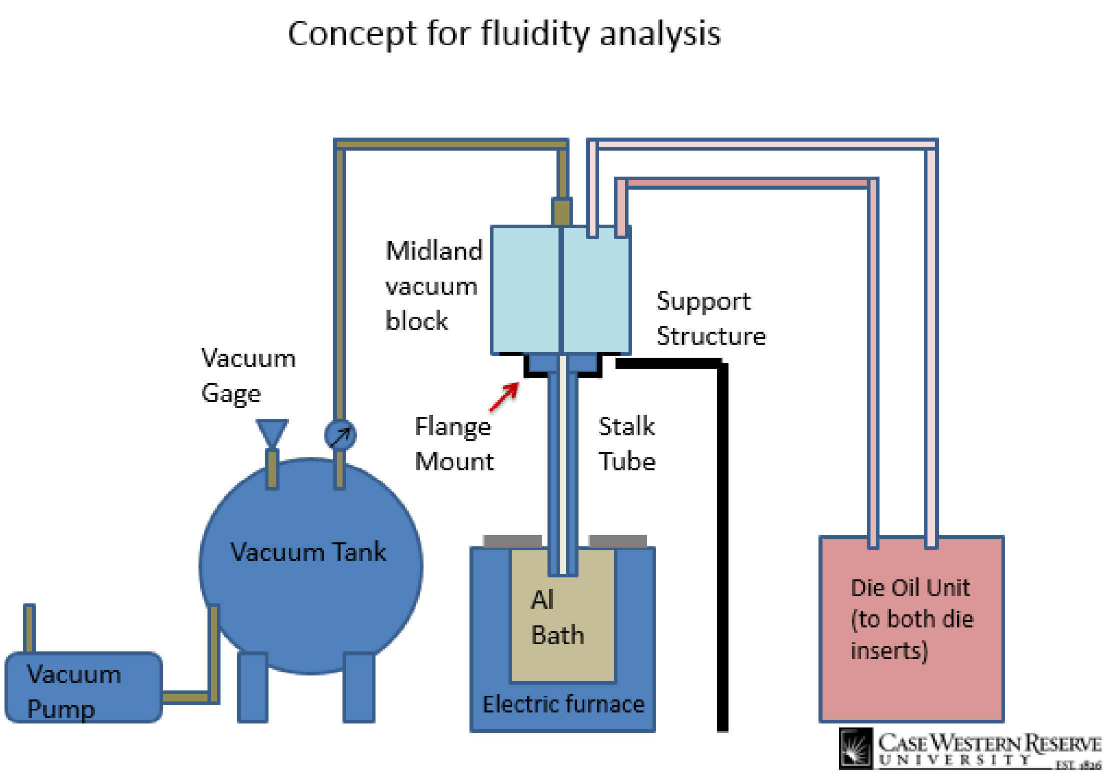

Figure 4.1: Schematic for fluidity test based on vacuum suction into thin walled *mold*

The center piece of this system is the Midland vacuum block, also known as the Midland vent block. Used to apply vacuum to a cavity, this block has multiple "zig-zag" steps forcing the molten metal to flow in a very thin-wall section until it freezes. The hypothesis is such a flow pattern will differentiate well among alloys with varying fludity.

Everything else being the same, an alloy with the highest fluidity should flow furthest. Other parts of the system shown in the figure include (from left to right) a vacuum pump and vacuum tank used to generate vacuum; a vacuum gage that measures the vacuum level in the tank and allows the application of the same vacuum throughout all the experiments; the Midland vent block; a silicon riser tube attached to the vent block with a gasket, so as to prevent air leaks; a crucible with molten aluminum alloy kept at a desired temperature by an electrical pot furnace; an oil die heater that circulated hot oil at a pre-set temperature through the vent block. Accurate temperature control of the vent block is critical, since the vent block temperature can affect the experimental results.

The vent block is mounted on rails and sits on a vertically-movable platform as illustrated in Figure 4.2.

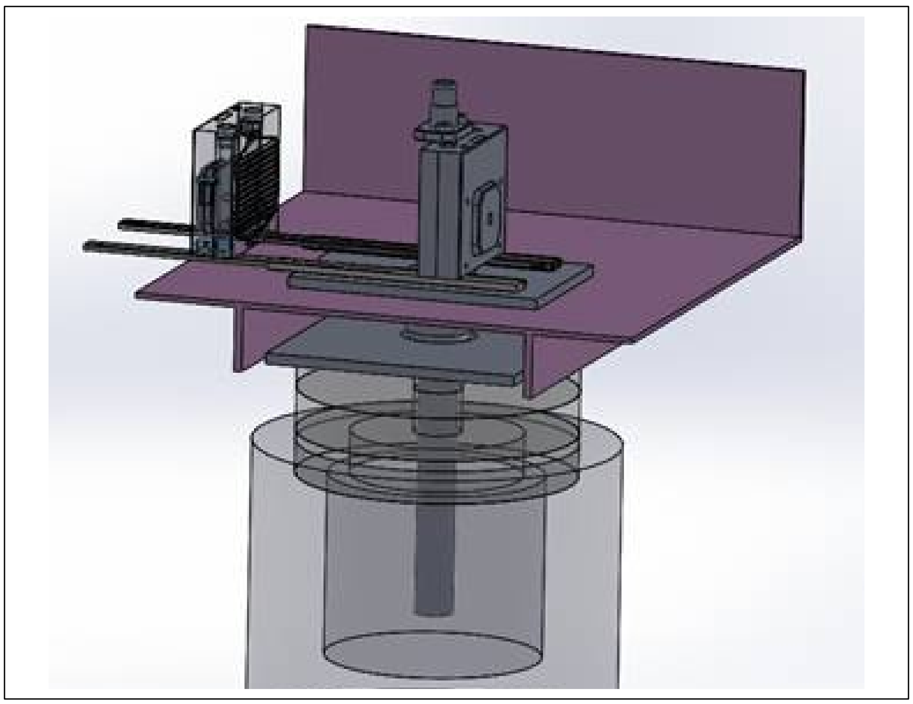

Figure 4.2: Movable vent block

A typical experiment starts by closing the two halves of the vent block, placing the sealing gasket on the top end of the riser tube and lowering the entire platform with the vent block until it sits tight on the silicon carbide riser tube. While this is done, the vacuum pump will gradually bring the vacuum level in the vacuum tank to the required level. At this point a valve is opened, connecting the vacuum tank to the top of the vent block. The molten aluminum is sucked by the vacuum into the vent block. All other variables being the same, a high-fluidity alloy tends to fill the vent block more. Controlled variables include:

- Molten metal temperature (with furnace controller)
- Riser tube temperature (with temperature controlled coil heater around the tube)
- Vent block temperature with oil die heater

The individual components of the fluidity measurement system are illustrated in the following figures:

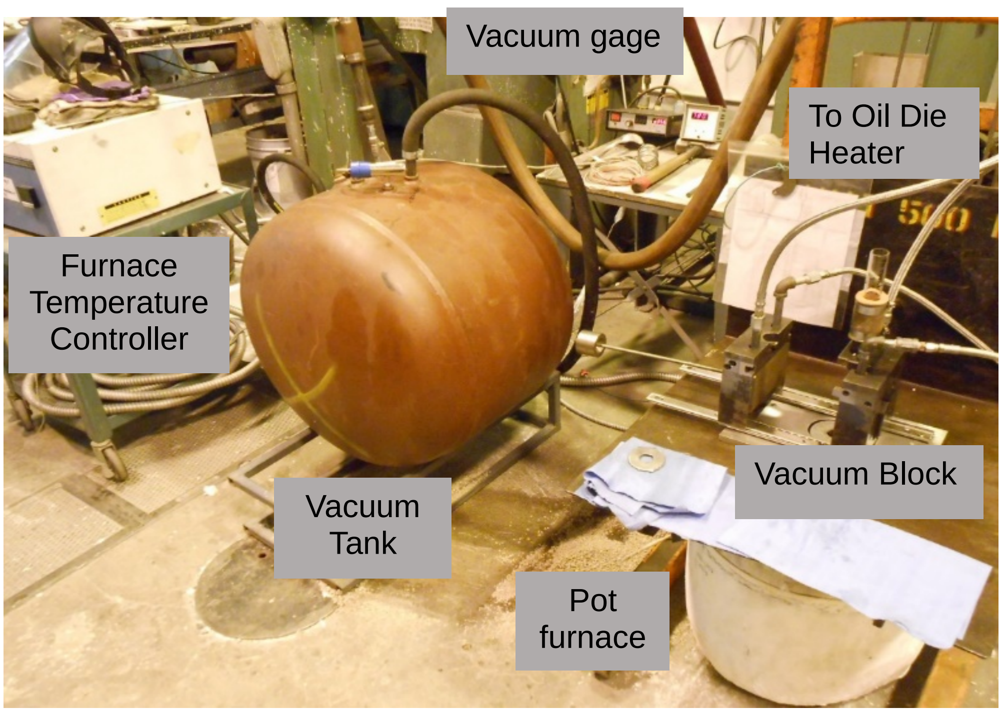

Figure 4.3: Fluidity measurement system

Figure 4.4: Open vent block mounted on rails; vacuum sealing gaskets

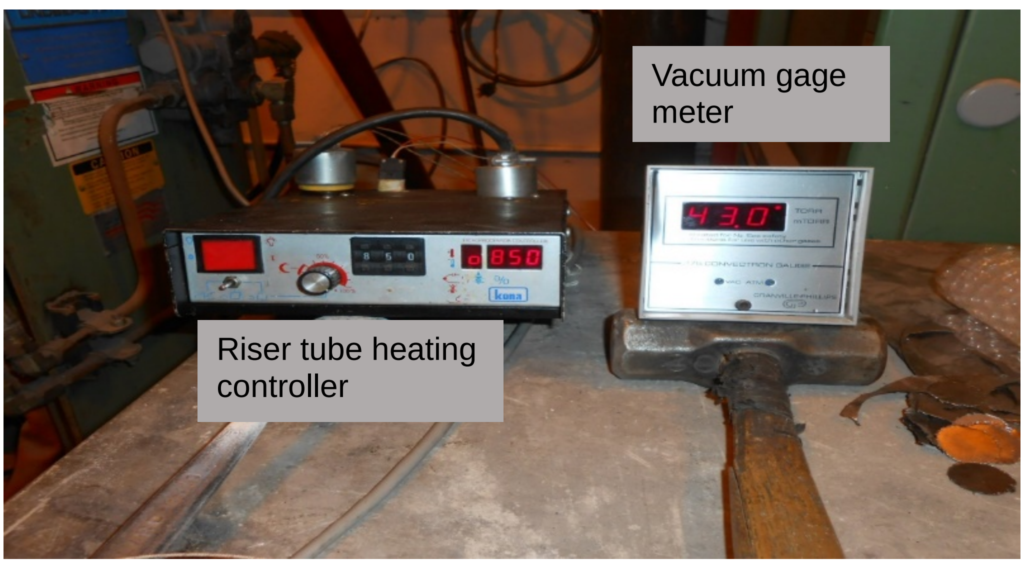

Figure 4.5: Riser tube heater controller and vacuum gage meter

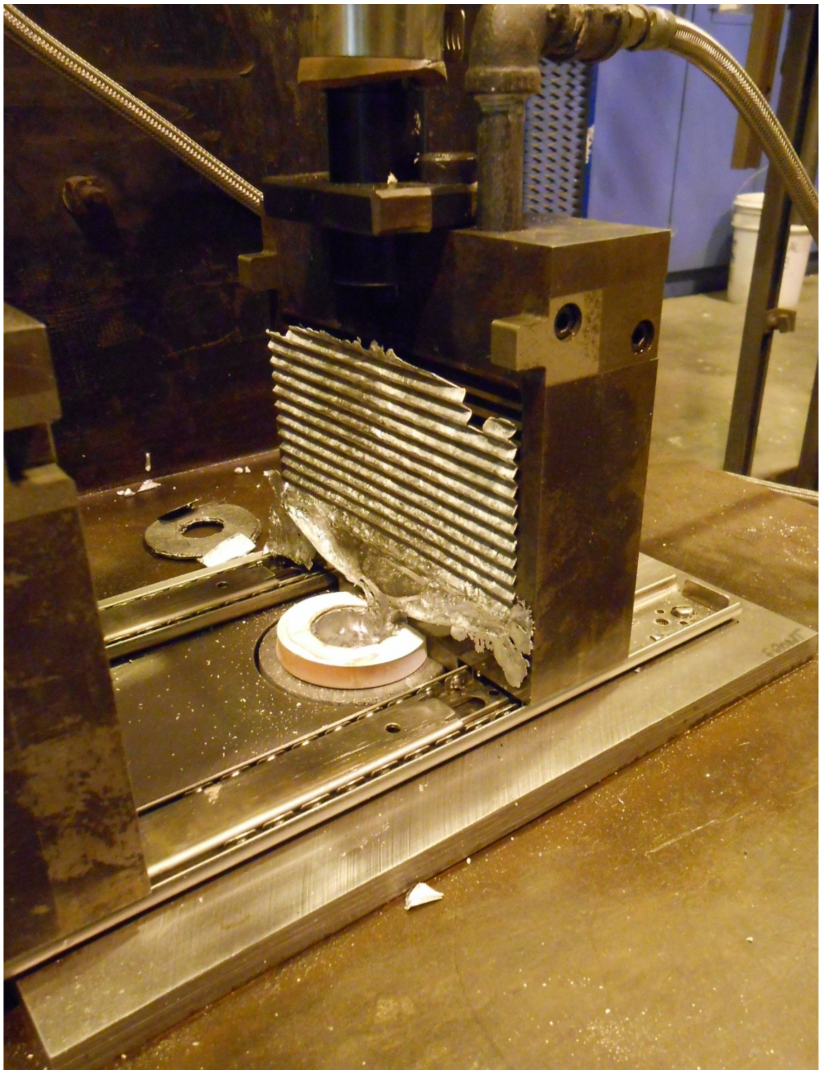

Figure 4.6: Open vent block demonstrating filling with aluminum

When the molten metal has high fluidity, it sometimes fills the entire vent block. To avoid a situation where the block is not large enough to distinguish between alloys with high fluidity (as they would all reach the top of the vent block) a larger vent block was procured. A schematic of the new vent block is illustrated in Figure 4.7. A picture of the installed vent block is shown in Figure 4.8.

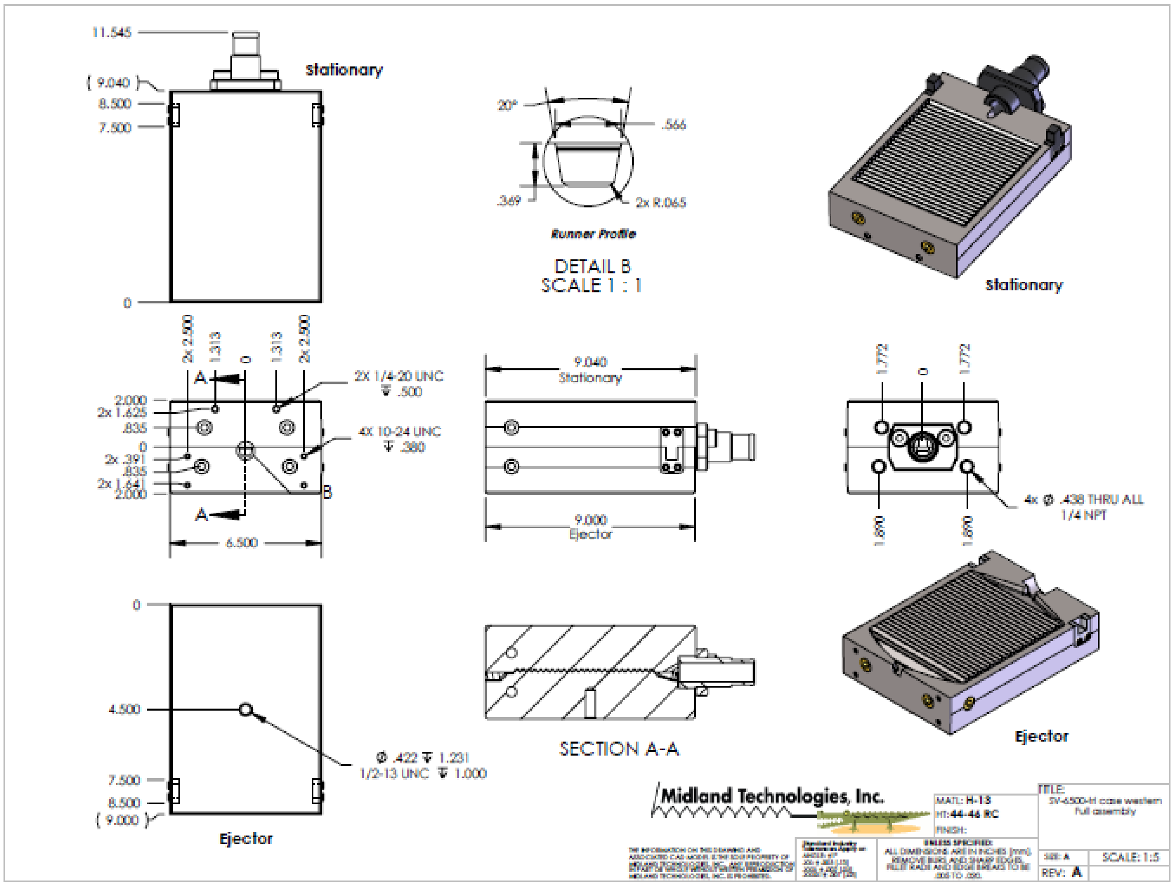

Figure 4.7: Schematics of the large vent block

Figure 4.8: Installed large vent block side-by-side with old vent block

The new vent block is almost twice as high. This should allow the measurement of behavior of higher fluidity alloys.

Fill Velocity

An experiment was conducted to determine the velocity of the incoming metal into the vent block. To this end, a vertical tube was attached to the bottom of the vent block, with two horizontal wires, placed 2 inches apart. The wires were connected to an osciloscope. As the vacuum is applied to the top of the vent block, the incoming molten metal rushes into the vent block while shorting the two wires. The set-up is illustrated in Figure 4.9. The time it takes the metal to flow beteen the wires is recorded and used to calculate the velocity.

According to the measurements taken from this experiment and illustrated in Figure 4.10, the incoming molten metal velocity is 416 ft/sec. This velocity is in line with injection velocity in die casting.

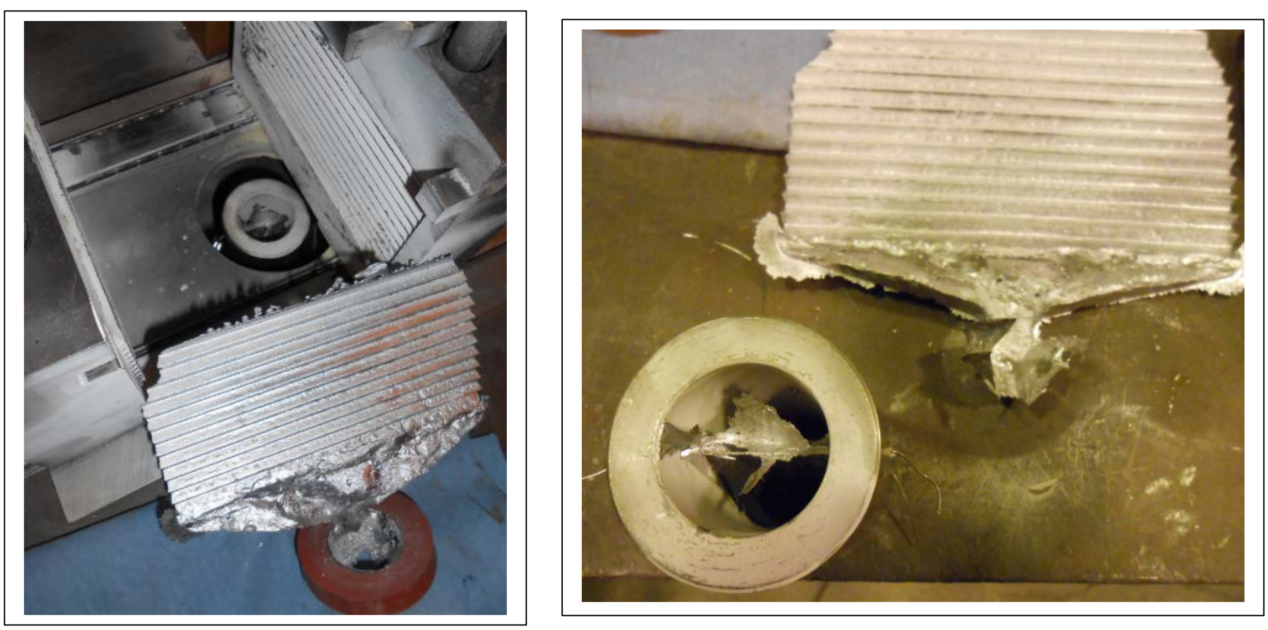

Figure 4.9: Set-up for fill velocity measurement

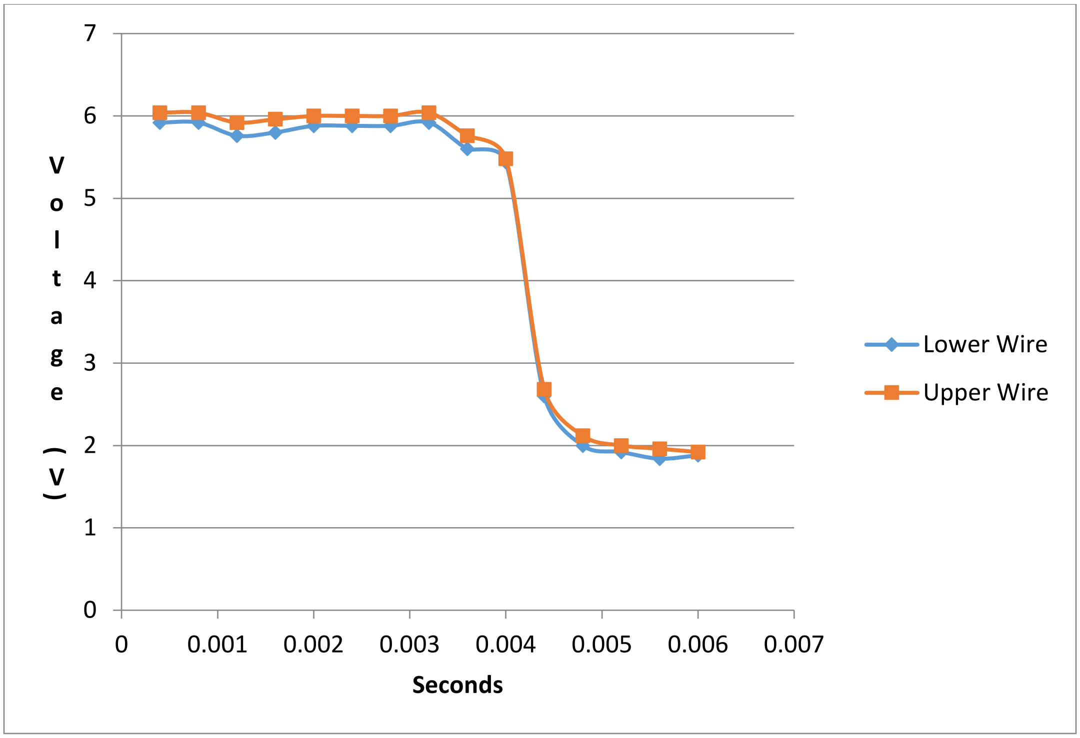

Figure 4.10: Time to fill used to determine fill velocity

Pax-It Image Analysis

To quantify fluidity, a measurement of the filling was required. Initially, the filling distance was considered. However, the castings are two-dimensional and did not always have straight edges. Often, the center of the castings filled more than the edges. The surface area of the casting was selected as a better parameter. The Pax-It image analysis was used to quantify this surface area. The following procedure was employed:

- First the image needs to be calibrated to the correct length
- The ruler in the images helps measure the length of the image and check calibration settings
- Finally, the projected area of the fluidity experiments was calculated using the Pax-It image analysis software as illustrated in Figure 4.11.

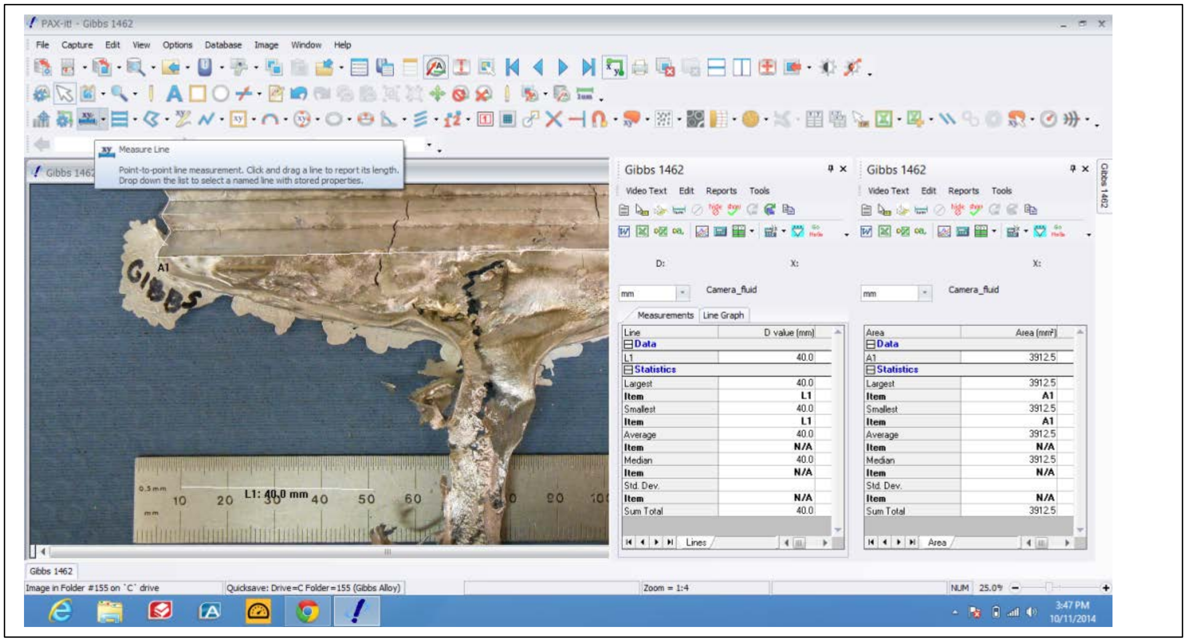

Figure 4.11: Pax-It shot screen #1

After the image is properly calibrated, the polygon area tool is used to trace the image. This will calculate the total area of the 2-D image when the image is traced as illustrated in the shot screen shown in Figure 4.12.

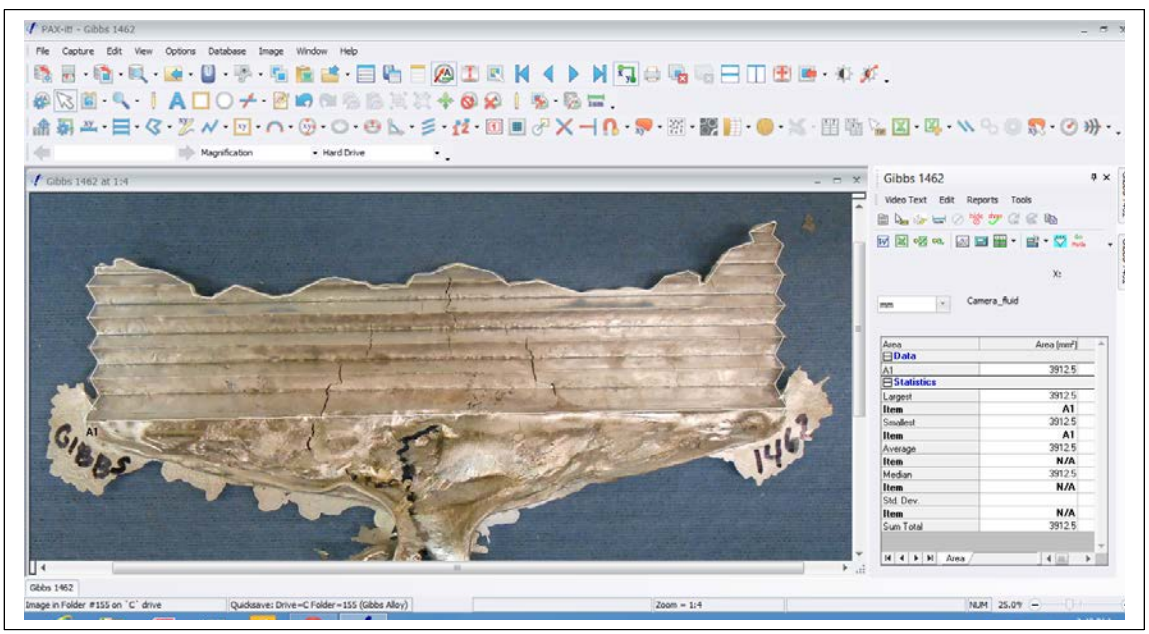

Figure 4.12: Pax-It shot screen #2

5. Results and Discussion

5.1 Fluidity Experiments

A benchmarking test was initially conducted with the aluminum 356 alloy by varying the molten metal temperature. The anticipated change in fluidity with temperature was well captured by the test, as illustrated in Figure 5.1.1 that shows the castings and Figure 5.1.2 that shows a plot of the casting area as a function of temperature. A fluidity test was conducted with the aluminum 380 alloy by varying the molten metal temperature. The change in fluidity with temperature is illustrated in Fig 5.1.3. The area of the foil increases as a function of temperature as shown in the plot in Figure 5.1.4.

Figure 5.1.1: Thin foil of 356 alloy solidified in the vent block: the area of the foil increases as a function of temperature and provides a sensitive measure of fluidity

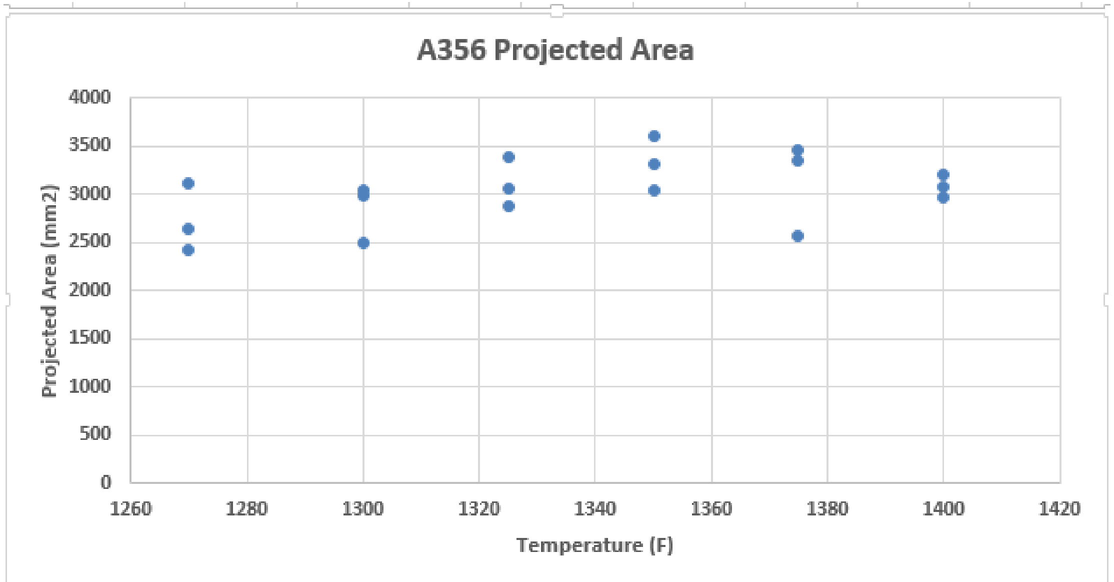

Figure 5.1.2: Projected area of A356 castings as a function of temperature

Figure 5.1.3: Thin foil 380 alloy solidified in the vent block: the area of the foil increases as a function of temperature

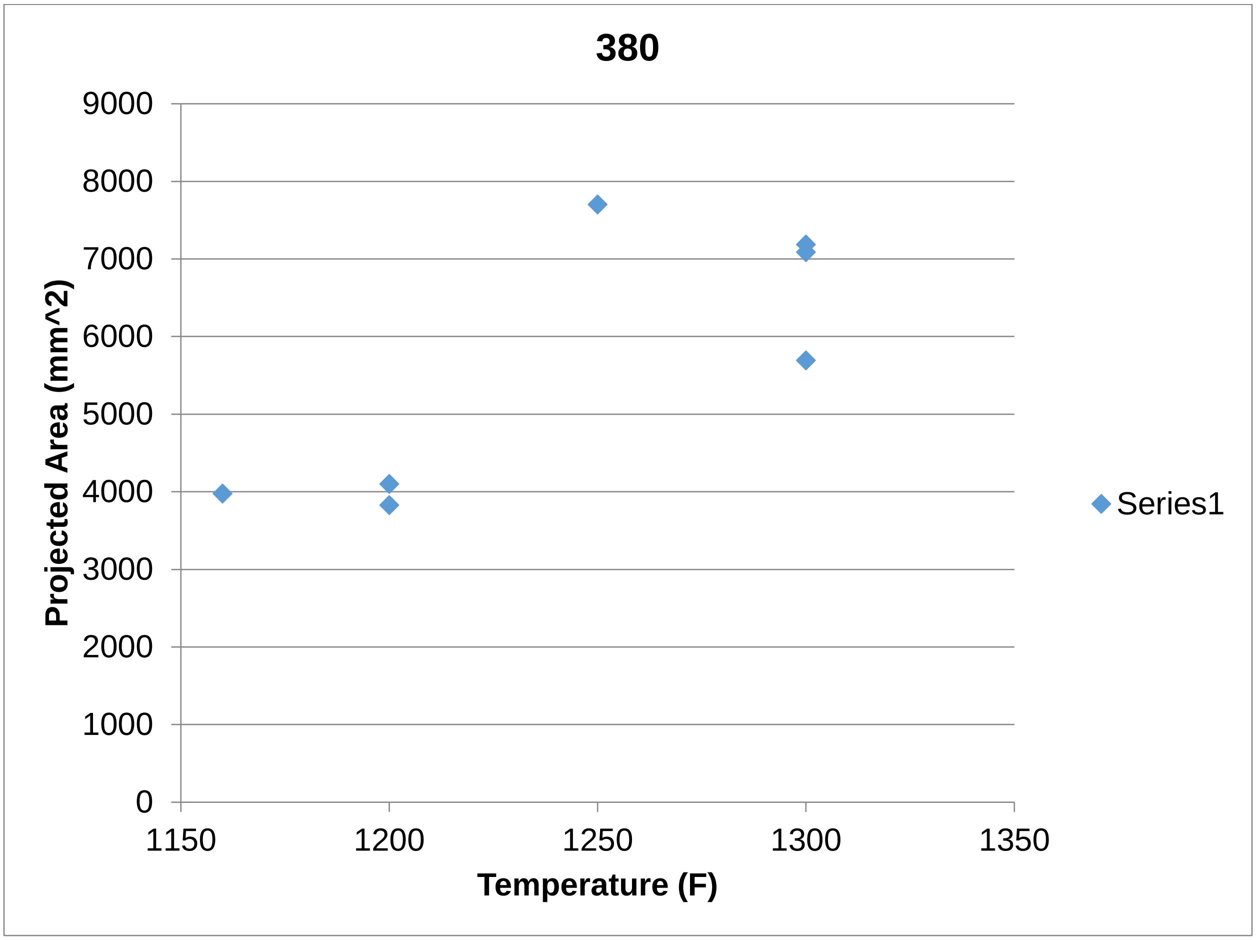

Figure 5.1.4: The area of the 380 alloy cast foil increases as a function of temperature

5.2 Fluidity of alloys with modified compositions

With a method to measure fluidity in place, the focus of the experimental work was shifted to testing alloys with modified compositions expected to increase fluidity. Based on evidence from literature, increasing the copper content of high-silicon alloys such as 390 held good promise to increase fluidity. These alloys are not commerically available and had to be prepared in the laboratory. The aluminum-copper phase diagram, illustrated in Figure 5.2.1, shows mutual solubility of copper in liquid aluminum up to fairly high percentages.

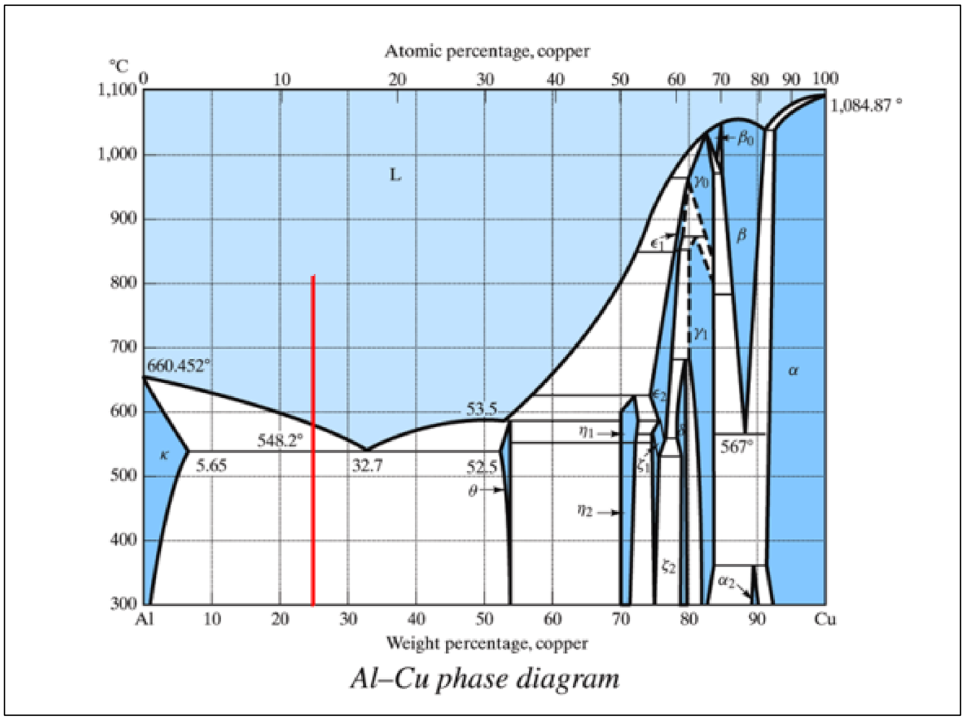

Figure 5.2.1: Al-Cu phase diagram

Initially, we tried adding copper to molten 390 alloy in the resistance furnace we use for the fluidity experiments. While convenient, this approach did not work. The copper addition did not dissolve properly and the copper concentration in the alloy did not increase significantly. To ensure proper chemistry a more elaborate approach to alloying was required:

1. Melting a 390 alumium charge in the 350kW induction furnace; adding the copper
2. Checking the composition
3. Repeating this process untill the correct composition is obtained

Melting in the induction furnace allows heating to higher temperatures. In addition, the metal is stirred by the electromagnetic field, thus facilitating better dissolution of the copper. Shown in Figure 5.2.2 is the Inductotherm power supply and induction furnace used to modify the 390 alloy. Discs of the modified alloys were cast in a permanent mold and surface machined to a flat, smooth surface appropriate for spectroscopic analysis. A spectromemeter at Empire Die Casting was used to conduct the analyses. The analysis was provided as in-kind cost-share to the project. The spectromemeter and a disc are illustrated in Figure 5.2.3 a, b below. The dark spots on the disc are the marks left by the spark used to evaporate alloy into the detector of the spectrometer.

Figure 5.2.2: Induction melting system used for adding copper to 390

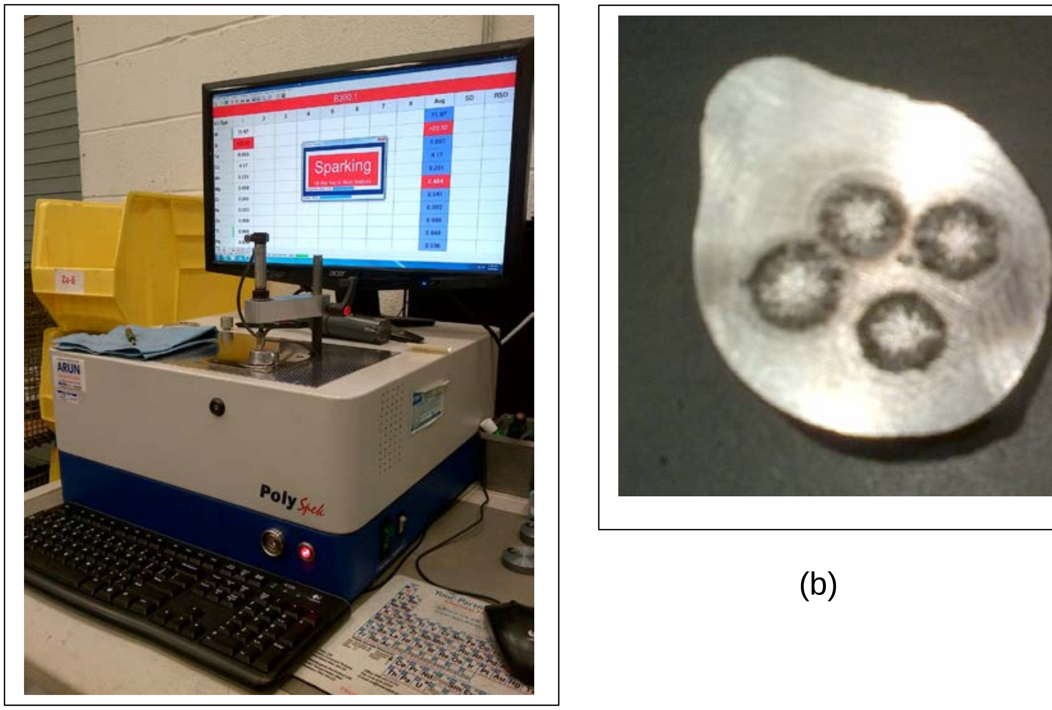

(b)

(a)

Figure 5.2.3: (a) Spectrometer at EDC used to analyze composition of modified alloys and (b) Typical cast aluminum alloy disc used for the analysis

The output of a typical analysis is illustrated in Table 5.2.1.

Table 5.2.1: Spectroscopic analysis of modified 390 aluminum alloy

Al	Si	Fe	Cu	Mn	Mg	Cr	Ni	Zn	Ti	Pb	Sn	Cd
72.61	>21.51	0.337	3.81	0.226	0.398	0.013	0.015	0.263	0.053	0.036	<0.001	<0.001
73.55	>20.70	0.358	3.75	0.231	0.426	0.014	0.018	0.115	0.05	0.036	0.015	0.003
74.95	>19.14	0.367	3.87	0.244	0.467	0.016	0.015	0.105	0.049	0.036	0.009	0.001

The modification trials for increasing the amount of copper in the 390 alloy indicate a yield of approximately 50%. In other words, only about half of the copper goes in solution. It is typical in alloying to have lower than 100% yield. The yield can vary from element to element.

Modified 390 alloys with 2% and 4% copper additions were prepared and the fluidity tested. The baseline composition of the 390 alloy is illustrated in Table 5.2.2 .

Table 5.2.2: Baseline composition of the 390 alloy

Al	75.2 - 79.6 %
Cu	4.0 - 5.0 %
Fe	<= 0.50 %
Mg	0.45 - 0.65 %
Mn	<= 0.10 %
Si	16 - 18 %
Ti	<= 0.20 %
Zn	<= 0.10 %

Silicon and copper have been reported as fluidity promoters in aluminum alloys.

Additional fluidity tests were conducted with the modified 390 aluminum alloys 390-1, 390-2, 390-3 alloys. The target composition of these modified 390 alloys includes additions of 2%, 4%, and 6% of silicon respectively. The results are shown in Figures 5.2.4-5.2.9.

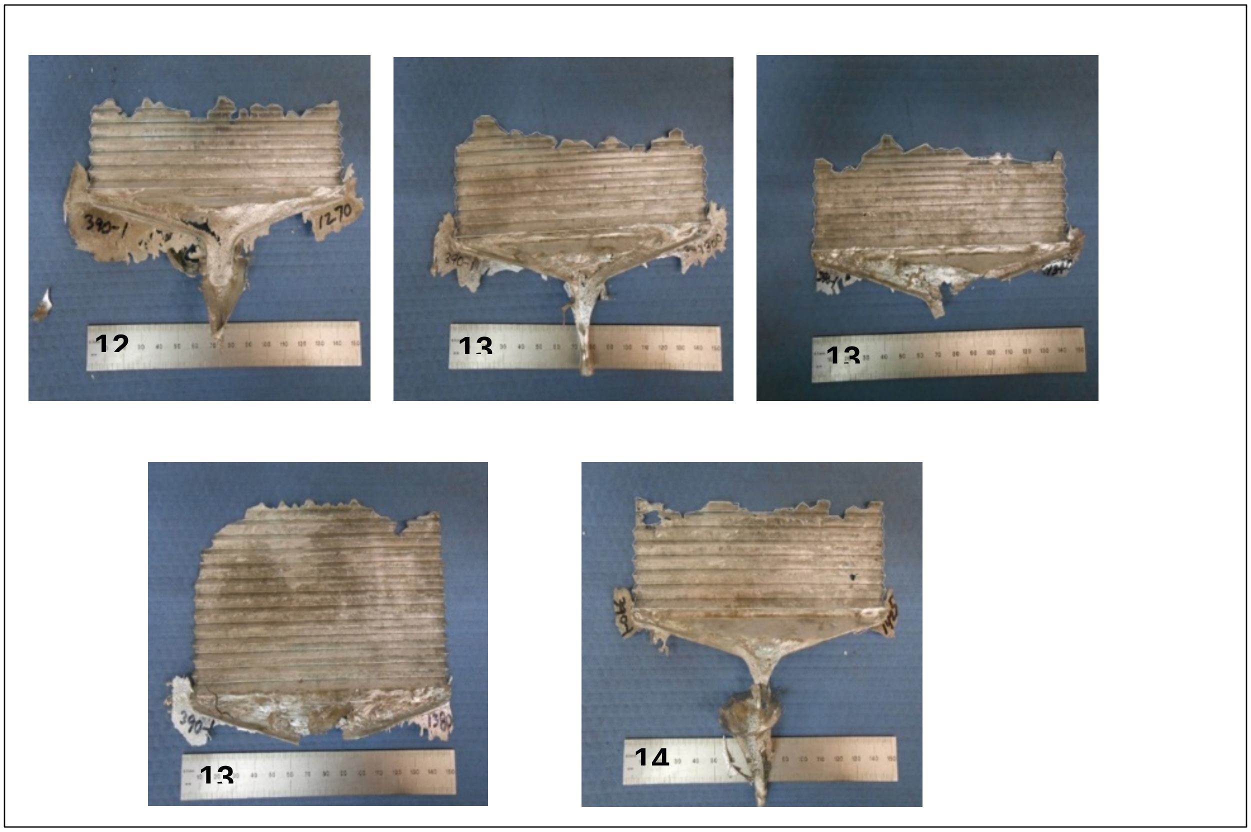

Figure 5.2.4: Thin foil 390-1 alloy solidified in the vent block: the area of the cast aluminum foil increases as a function of temperature

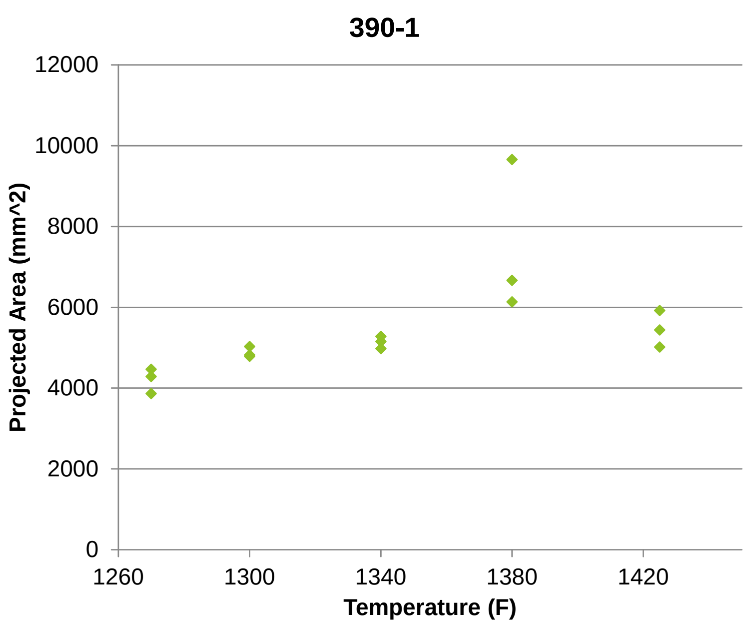

Figure 5.2.5: The area of the 390-1 alloy cast foil increases as a function of temperature

Figure 5.2.6: Thin foil 390-2 alloy film solidified in the vent block

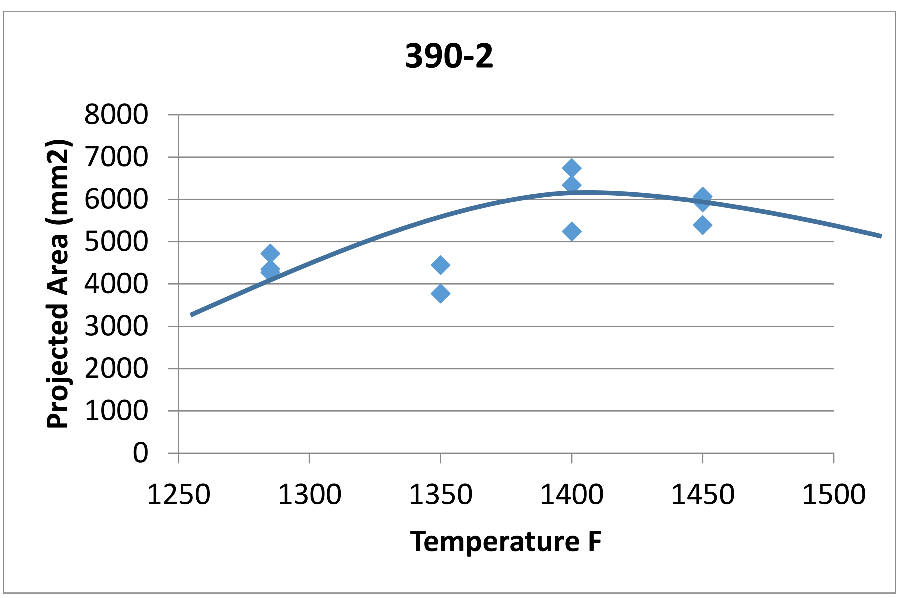

Figure 5.2.7: The area of the 390-2 cast alloy as a function of temperature

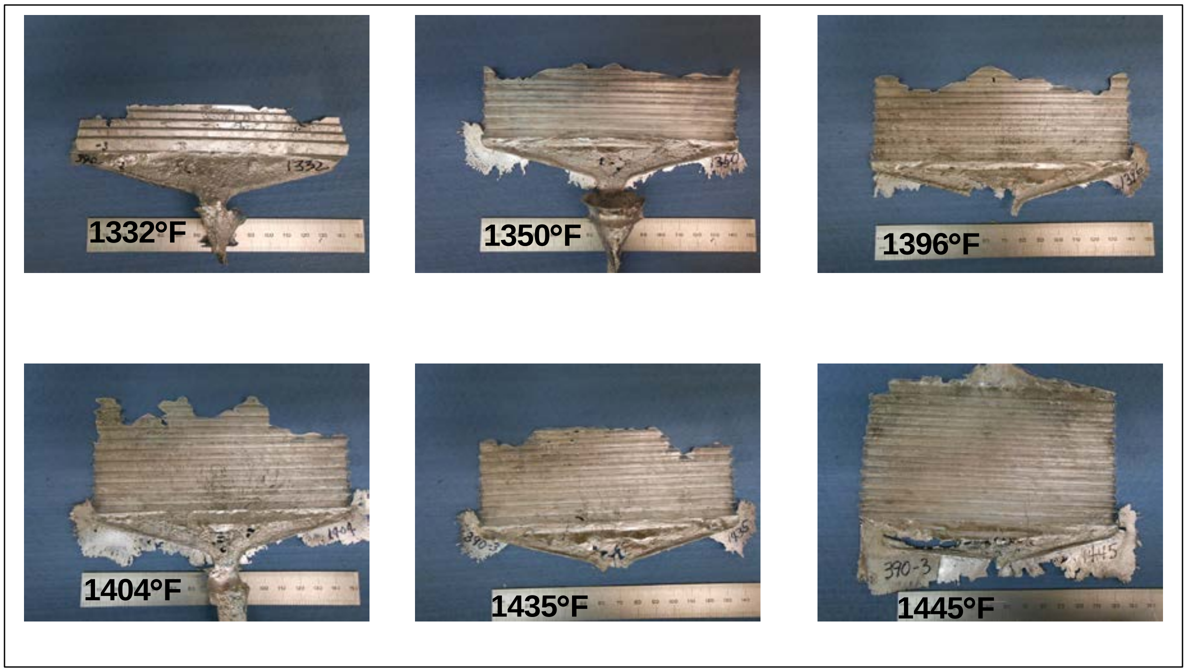

Figure 5.2.8: Thin foil 390-3 alloy film solidified in the vent block

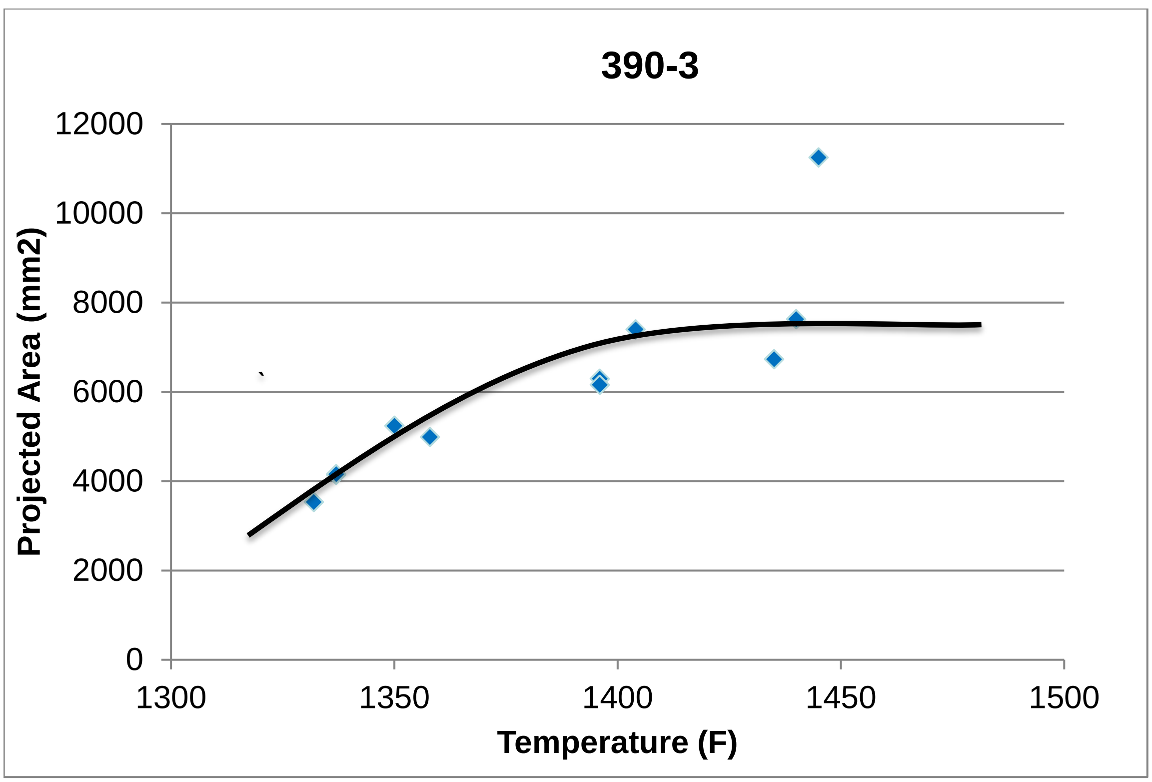

Figure 5.2.9: The area of the 390-3 alloy cast foil increases as a function of temperature

Table 5.2.3 and the respective bar graph in Figure 5.2.9 illustrate the increase in fluidity obtained by additions of Si and Cu to the base 390 alloy. While there is an improvement trend, the changes in fluidity are rather small.

. **Table 5.2.3:** Fluidity of 390 modified with additions of Si and Cu

	Average Values	Std Dev
Si+2%	7879	545
Si+6%	8048	1718
CU +6%	9071	519
390 Only	6939	1408

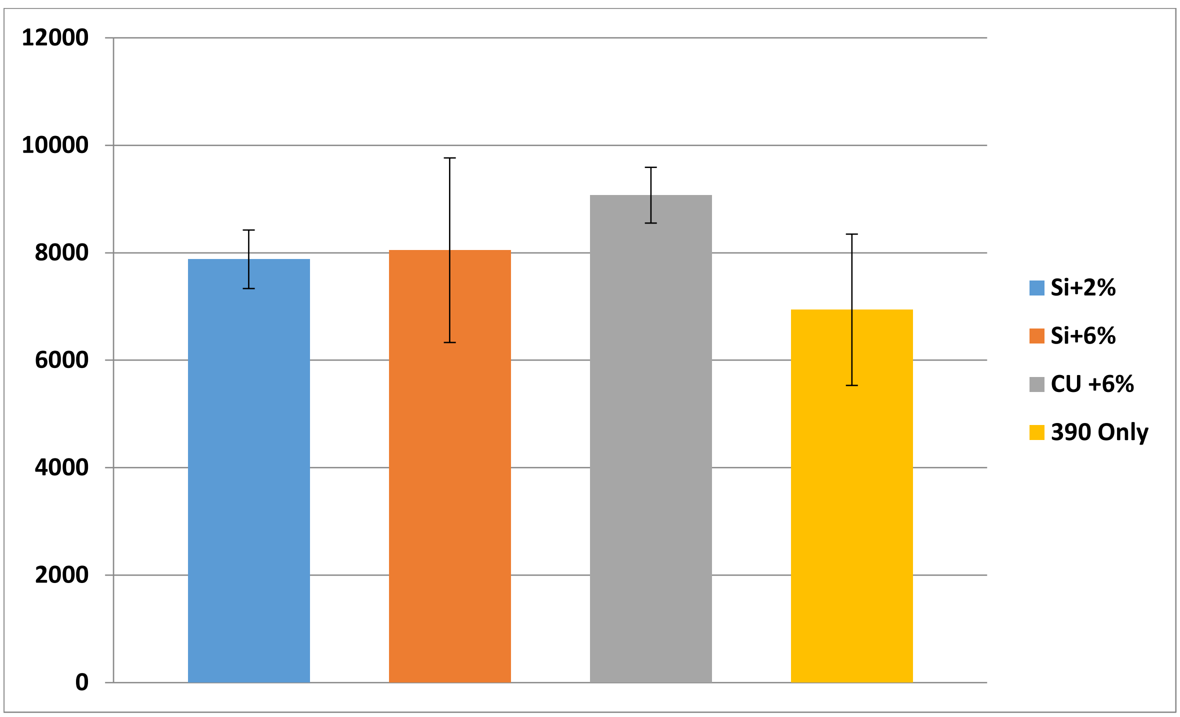

Figure 5.2.9: Increase in fluidity obtained by additions of Si and Cu to 390

Additional fluidity experiments were carried out with A380 alloy using a BN-coated vent block. The results are shown in Figures 5.2.10 and 5.2.11. Coating the vent block with BN markedly increased fluidity and filling.

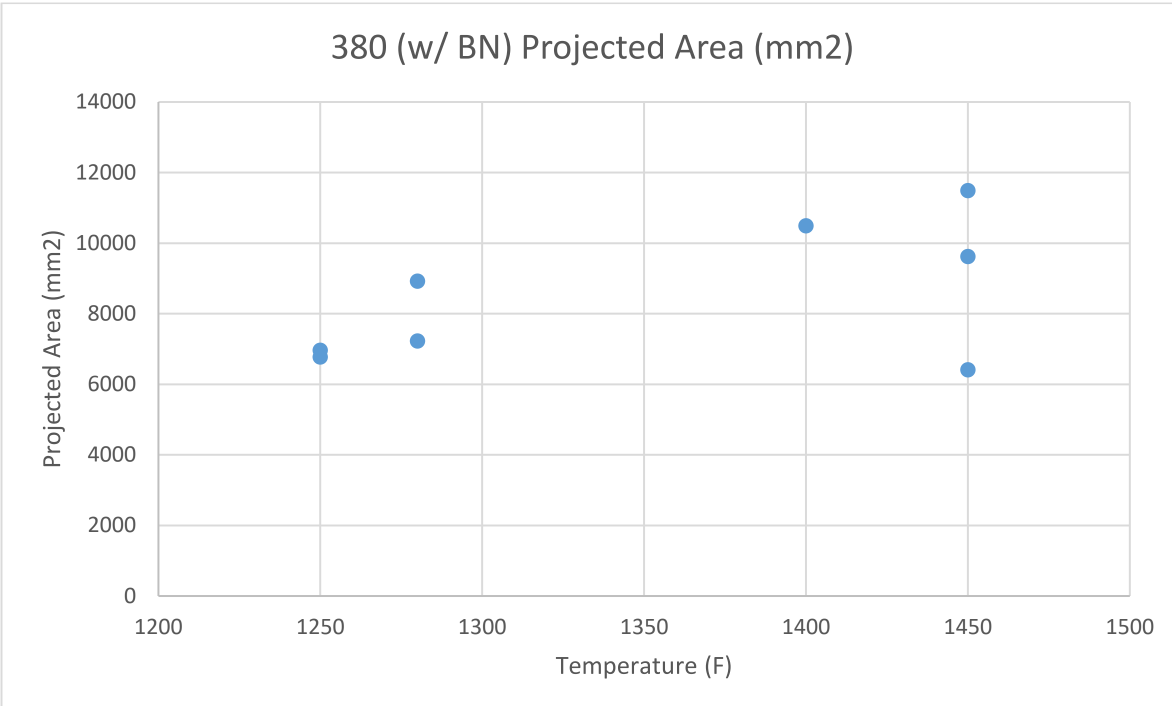

Figure 5.2.10: Fluidity of A380 using a BN-coated vent block

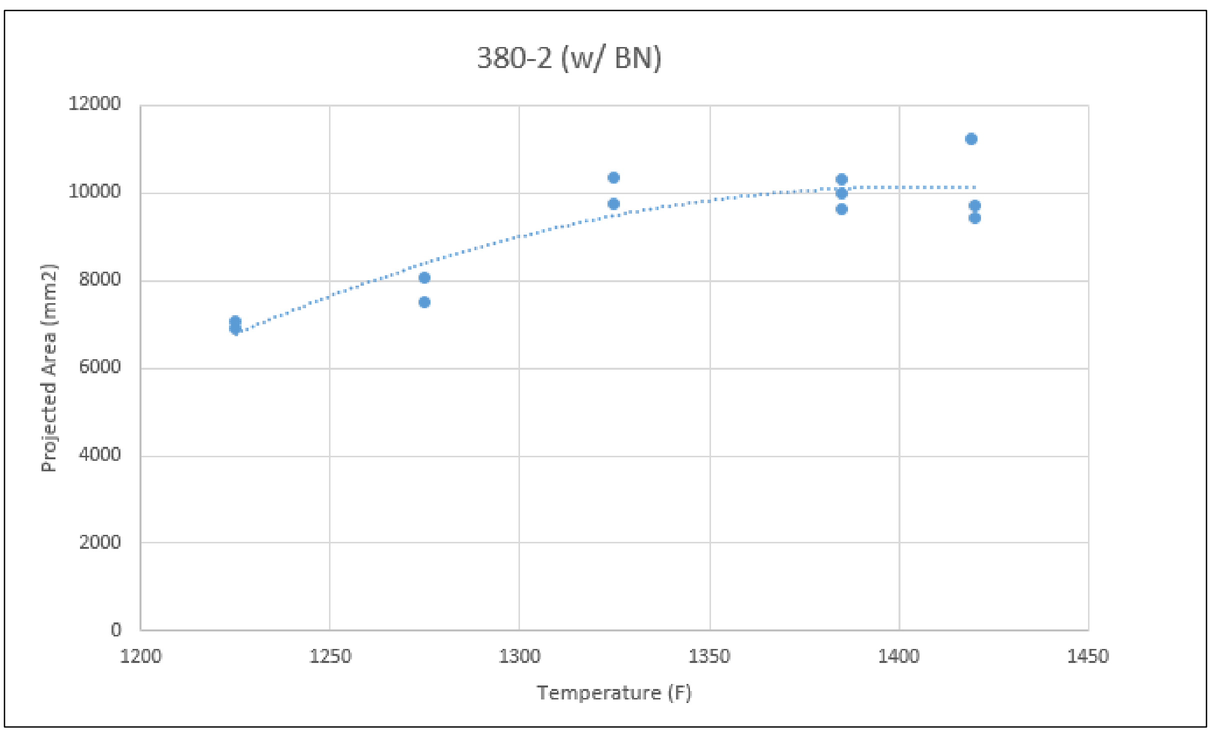

Figure 5.2.11: Fluidity of A380-2 using a BN-coated mold

5.3 Mechanical Testing

The mechanical properties of test bars die cast at Premier Die Casting were measured and are reported. The alloys tested are listed below and composition of the alloys employed is listed in Table 5.3.1.

- 390 Lo Fe- 16% Si Target
- 390 Lo Fe- 18% Si Target
- 390 Lo Fe- 20% Si Target
- ALMG2MN
- Gibbsalloy

Table 5.3.1: Composition of the alloys die cast at Premier

Trial	# Shots	Alloy	Si	Fe	Cu	Mn	Mg
0	25	A380	9.18	0.77	3.24	0.21	0.251
1	40	Gibbsalloy MN	0.17	0.27	0.000	0.89	2.98
2	40	ALMG2MN	0.32	0.51	0.014	0.66	2.48
3	40	390 LoFe-1	15.59	0.31	3.68	0.31	0.54
4	40	390 LoFe-2	17.49	0.32	3.95	0.28	0.51
5	40	390 LoFe-3	19.06	0.33	4.11	0.29	0.57

The results are listed in Tables 5.3.2-5.3.6 and summarized in Table 5.3.7.

Table 5.3.2: Mechanical properties of low iron 390 alloy with 16% Si

Sample Information:

Name	Value
Alloy	390 Lo Fe- 16% Si Target (Trial 3)
Heat Treat	F – 16 Days of Natural Aging
Process	HPDC (R1)

Specimen Results:

Spec #	Shot #	Cav #	Bar Ø (in)	Yield (ksi)	UTS (ksi)	Elong (%)	E Mod (ksi)
1	3-20A	1	0.247	31.1	39.1	0.852	12239
2	3-21A	1	0.247	31.4	38.9	0.821	12127
3	3-18B	2	0.245	32.2	40.7	0.899	14043
4	3-15B	2	0.245	32.2	40.5	0.875	13577
5	3-17A	1	0.247	31.5	39.3	0.870	11967
6	3-16B	2	0.245	31.9	40.7	0.887	14133
7	3-15A	1	0.247	31.6	38.7	0.827	11767
8	3-19A	1	0.247	31.2	39.7	0.894	12277
9	3-41B	2	0.245	32.7	41.4	0.957	12910
10	3-13B	2	0.245	32.7	38.8	0.767	12284
11	3-21B	2	0.245	32.6	40.0	0.860	12785
12	3-41A	1	0.247	31.6	38.4	0.813	11531
13	3-19B	2	0.245	31.9	43.4	1.132	13625
14	3-16A	1	0.247	32.1	36.8	0.702	11446
15	3-14B	2	0.245	32.4	39.5	0.810	13604
16	3-18A	1	0.247	31.6	43.6	1.239	11684
17	3-14A	1	0.247	31.6	42.1	1.041	12701
18	3-20B	2	0.245	32.5	40.7	0.917	12903
19	3-17B	2	0.245	32.8	38.8	0.774	12180
20	3-13A	1	0.247	32.0	41.6	0.997	11807
Mean				**31.9**	**40.2**	**0.903**	**12601**
Std. Dev.				**0.5**	**1.7**	**0.127**	**859**

Table 5.3.3: Mechanical properties of low iron 390 alloy with 18% Si

Sample Information:

Name	Value
Alloy	390 Lo Fe- 18% Si Target (Trial 4)
Heat Treat	F – 16 Days of Natural Aging
Process	HPDC (R1)

Specimen Results:

Spec #	Shot #	Cav #	Bar Ø (in)	Yield (ksi)	UTS (ksi)	Elong (%)	E Mod (ksi)
1	4-47A	1	0.247	33.6	40.5	0.851	11979
2	4-46A	1	0.247	33.3	34.1	0.523	11780
3	4-48B	2	0.245	34.6	42.1	0.942	12453
4	4-10B	2	0.245	35.0	39.9	0.726	12423
5	4-45A	1	0.247	33.1	39.5	0.809	11778
6	4-39B	2	0.245	33.2	41.1	0.885	13945
7	4-10A	1	0.247	34.3	38.8	0.700	12097
8	4-47B	2	0.245	34.3	41.0	0.837	12590
9	4-41A	1	0.247	33.1	41.5	0.977	11490
10	4-46B	2	0.245	34.0	41.4	0.895	13211
11	4-11A	1	0.247	33.2	37.0	0.632	12245
12	4-48A	1	0.247	33.7	39.3	0.752	12033
13	4-40B	2	0.245	33.6	37.7	0.650	13112
14	4-39A	1	0.247	32.9	35.3	0.562	12210
15	4-12B	2	0.245	34.0	37.2	0.639	12007
16	4-40A	1	0.247	33.1	37.6	0.682	11638
17	4-11B	2	0.245	33.9	40.2	0.833	12152
18	4-12A	1	0.247	33.3	38.0	0.677	12123
19	4-45B	2	0.245	33.7	38.7	0.716	12426
20	4-41B	2	0.245	33.4	37.2	0.631	12798
Mean				**33.7**	**39.2**	**0.758**	**12353**
Std. Dev.				**0.6**	**1.9**	**0.119**	**590**

Table 5.3.4: Mechanical properties of low iron 390 alloy with 20% Si

Sample Information:

Name	Value
Alloy	390 Lo Fe- 20% Si Target (Trial 5)
Heat Treat	F – 16 Days of Natural Aging
Process	HPDC (R1)

Specimen Results:

Spec #	Shot #	Cav #	Bar Ø (in)	Yield (ksi)	UTS (ksi)	Elong (%)	E Mod (ksi)
1	5-25B	2	0.245	36.1	36.6	0.479	14148
2	5-26A	1	0.247	****	34.0	0.417	12639
3	5-12B	2	0.245	****	35.6	0.460	12913
4	5-25A	1	0.247	****	35.1	0.461	12435
5	5-8A	1	0.247	36.0	36.7	0.520	12408
6	5-9A	1	0.247	36.4	37.1	0.529	12131
7	5-38B	2	0.245	****	35.4	0.450	13580
8	5-10B	2	0.245	35.4	37.0	0.494	15358
9	5-11A	1	0.247	35.8	36.6	0.516	12911
10	5-38A	1	0.247	****	35.5	0.484	12391
11	5-37A	1	0.247	35.8	35.8	0.497	12160
12	5-37B	2	0.245	36.3	36.5	0.492	12931
13	5-9B	2	0.245	36.0	37.4	0.518	13727
14	5-39A	1	0.247	****	34.8	0.450	12913
15	5-11B	2	0.245	35.2	36.7	0.510	13910
16	5-39B	2	0.245	****	35.1	0.434	12873
17	5-10A	1	0.247	34.6	36.5	0.493	12254
18	5-8B	2	0.245	35.3	36.2	0.471	14837
19	5-12A	1	0.247	35.7	37.3	0.563	12112
20	5-26B	2	0.245	35.5	36.4	0.473	15276
Mean				**35.7**	**36.2**	**0.489**	**13225**
Std. Dev.				**0.50**	**0.8**	**0.032**	**1056**

Table 5.3.5: Mechanical properties of low iron AlMg2Mn

Sample Information:

Name	Value
Alloy	ALMG2MN
Heat Treat	F (Natural age 20 Days)
Process	HPDC (R1)

Specimen Results:

Spec #	Shot #	Cav #	Bar Ø (in)	Yield (ksi)	UTS (ksi)	Elong (%)	E Mod (ksi)
1	2-21A	1	0.245	15.6	32.1	14.772	10916
2	2-46B	2	0.243	16.0	29.6	9.592	10182
3	2-48A	1	0.245	15.9	29.7	10.853	11405
4	2-43B	2	0.243	15.5	28.3	7.153	10628
5	2-45A	1	0.245	15.8	30.7	11.187	11046
6	2-46A	1	0.245	15.9	30.8	12.637	10382
7	2-47B	2	0.243	15.9	30.1	11.542	9782
8	2-23A	1	0.245	15.8	30.2	9.458	10175
9	2-22A	1	0.245	15.8	29.7	9.464	10287
10	2-48B	2	0.243	16.0	28.9	9.355	10996
11	2-24A	1	0.245	15.9	30.8	11.927	10357
12	2-44B	2	0.243	16.0	31.5	12.769	10082
13	2-45B	2	0.243	16.1	31.7	12.807	9911
14	2-24B	2	0.243	16.1	31.1	10.982	9296
15	2-21B	2	0.243	16.1	31.6	13.445	11038
16	2-43A	1	0.245	15.9	30.9	11.042	9906
17	2-23B	2	0.243	15.8	28.7	6.728	9859
18	2-22B	2	0.243	16.4	26.8	4.895	10506
19	2-44A	1	0.245	16.0	31.7	16.656	10680
20	2-47A	1	0.245	15.5	28.8	8.271	9964

Table 5.3.6: Mechanical properties of Gibbsalloy

Name	Value
Alloy	Gibbsalloy
Heat Treat	F (Natural age 20 Days)
Process	HPDC (R1)
NOTE	Cavity 1 (“A”) bars were all bent slightly during removal from ejector pins. Most were OK. But Yield Strength for cavity 1 and Elastic Modulus could be suspect given these facts. Specimen 1 data deleted from calculations. Specimen 7 & 14 removed for assignable causes.

Specimen Results:

Spec #	Shot #	Cav #	Bar Ø (in)	Yield (ksi)	UTS (ksi)	Elong (%)	E Mod (ksi)
1	1-64A	1	0.246	15.9	33.0	16.445	11644
2	1-66B	2	0.244	16.8	32.6	12.704	10337
3	1-59A	1	0.246	16.9	33.8	15.292	9513
4	1-63A	1	0.246	16.3	31.7	12.201	10241
5	1-56B	2	0.244	16.4	31.0	10.350	10204
6	1-64B	2	0.244	16.4	33.4	16.474	10527
7	1-58B	2	0.244	16.7	30.1	7.991	10228
8	1-56A	1	0.246	16.5	33.0	14.907	9814
9	1-59B	2	0.244	16.9	32.0	13.563	10515
10	1-57A	1	0.246	17.0	33.4	16.989	10080
11	1-60B	2	0.244	16.8	32.2	12.445	9907
12	1-55A	1	0.246	16.5	32.2	11.485	9483
13	1-65B	2	0.244	16.5	32.9	13.997	10534
14	1-55B	2	0.244	16.2	30.3	8.918	10422
15	1-58A	1	0.246	16.4	33.0	16.744	10074
16	1-60A	1	0.246	17.1	33.6	16.898	10675
17	1-63B	2	0.244	16.5	31.2	11.192	10384
18	1-66A	1	0.246	16.7	33.0	13.607	9668
19	1-57B	2	0.244	16.6	32.1	12.700	10525
20	1-65A	1	0.246	16.2	33.5	19.274	10107
Mean				**16.6**	**32.6**	**14.3**	**10152**
Std. Dev.				**0.26**	**0.82**	**2.46**	**371**

Table 5.3.7: Summary of mechanical properties

Alloy	Yield (ksi)	UTS (ksi)	Elong (%)	E Mod (ksi
390 Lo Fe- 16% Si Target	31.9	40.2	0.903	12,601
390 Lo Fe- 18% Si Target	33.7	39.2	0.758	12,353
390 Lo Fe- 20% Si Target	35.7	36.2	0.489	13,225
ALMG2MN	15.9	30.5	11.3	10,391
Gibbsalloy	16.6	32.6	14.3	10,152

5.4 Pull-Out Experiments with a Boron Nitride Coating on Rough Surface Pins

Heat transfer at the interface of the solidifying metal with the mold as well as the die surface roughness have been identified as an important factors in the ability of the metal to fill the cavity. Anecdotal evidence points at better filling obtained dies with a textured surface compared with a smooth die surface. One plausible cause is better retention of the die lubricant by the textured surface. Yet another possibility is that an insulating air gap forms between the molten metal and the die. The air gap slows down the heat transfer from the molten metal to the die steel, thus promoting better filling. The following experiments were carried out to confirm these hypotheses.

A potential method of introducing controlled roughness in the surface of die casting dies is shot peening. Metalife™ is a shot peening process that has been offered exclusively to the die casting industry by Badger Metals Tech, primarily to introduce compressive stresses in the surface. A side benefit of the process is a rough surface finish.

To quantify the roughness caused by the Metalife™ process, H13 pins have been procured and provided to Badger Metals for processing. The company has agreed to provide the treatment as cost share to the project. The shot-peened rods were prepared for a pull-out experiment to find out by how much the pull-out load increases if the BN coating is not reapplied. This detail is important for the coating to be practical as a semi-permanent solution. In other words, the BN would be applied once every hour, or once every shift rather than every single shot. The purpose of the shot peening is to retain more of the coating material on the pull out rods/dies. If the surface is smooth, the semi-permanent coating would more likely be “stripped” every time the casting is ejected.

0.25” dia. pull-out rods were shot peened by Badger Metals Tech using the Metalife™ process. Badger Metals provided this service as cost share to the project. The Metalife™ process is widely used by die casters to introduce compressive stresses in the surface of the die.

Figure 5.4.1 shows a textured pull-out rod. Note the “matt” appearance in the textured section of the rod, compared to the shinny end.

Figure 5.4.1: Textured pull-out rod

The rod was coated with BN, as shown in Figure 5.4.2.

Figure 5.4.2: BN coated pull-out rod

The coated rod was then tested with the pull-out test on a #500 bench tester. In the first test, the load required to pull out the rod was low, on the order of #150. After the test, the coating seemed in good condition, although not entirely intact. The asperities (ridges) in the textured surface appeared to have lost most of the BN, while the valleys were still filled with BN as illustrated in Figure 5.4.3a. Note the slight spalling of the BN at the melt line in the close-up 5.4.3b.

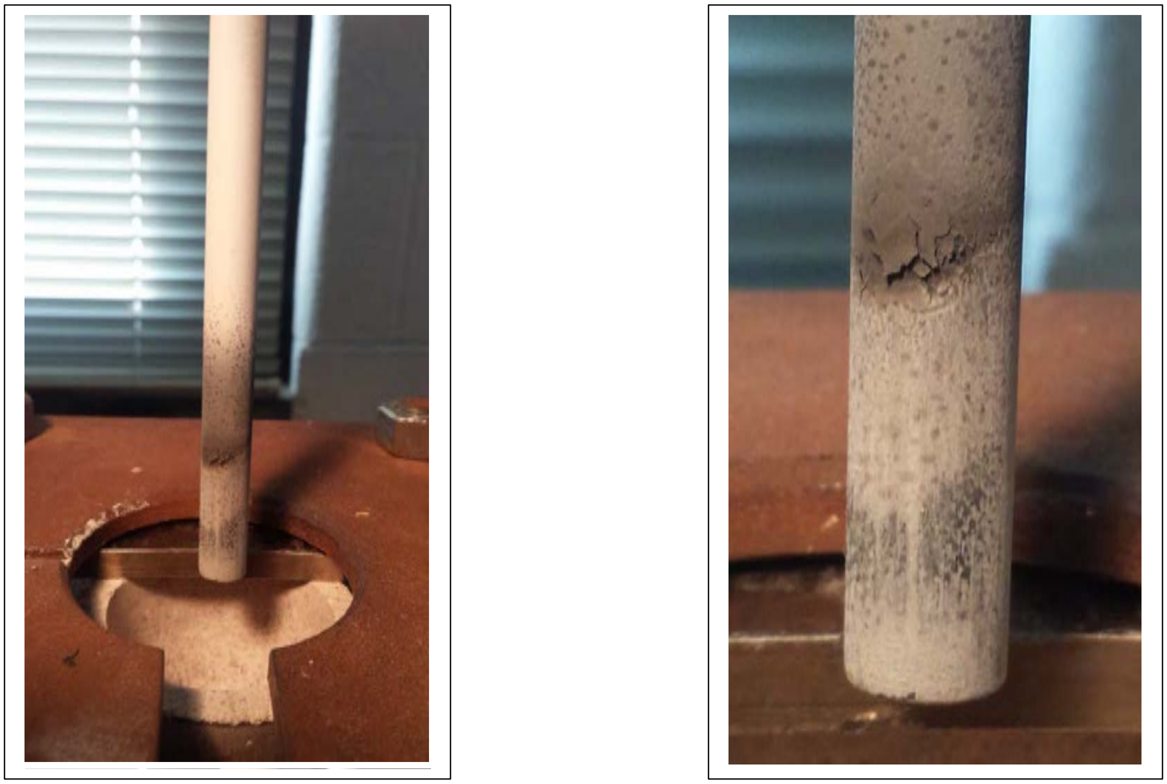

Figure 5.4.3:(a) Rough rod after first pull-out (b) close-up

Another experiment was conducted with this rod without recoating it. The pull-out load was still below #500. The pull-out plots for first (a) and the second (b) pull-out experiments are shown in Figure 5.4.4(a) and (b) respectively.

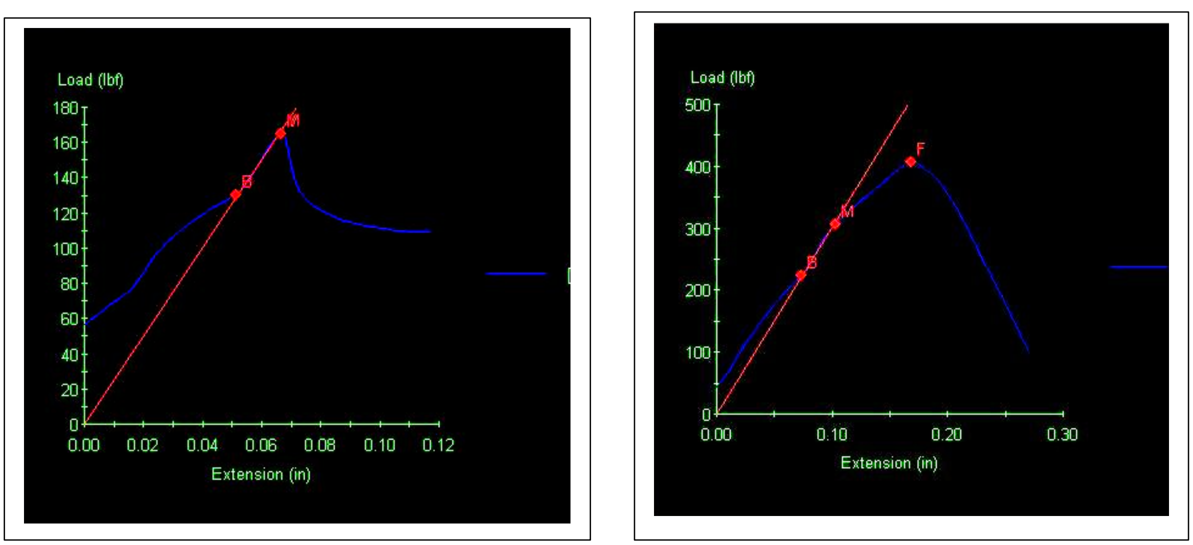

Figure 5.4.4: Pull-out plots for the rough surface rod (a) first pull-out (b) second pull-out

The pull-out experiment was repeated with a smooth surface rod. The first pull-out test showed even lower release load, less than #10. Upon inspection of the coating, the low end of the rod seemed to have been stripped entirely. See Figure 5.4.5. Running the test a second time with this rod did not allow pull-out under the max load of #500 applied by this test rig.

Figure 5.4.5: Smooth surface rod after first pull-out

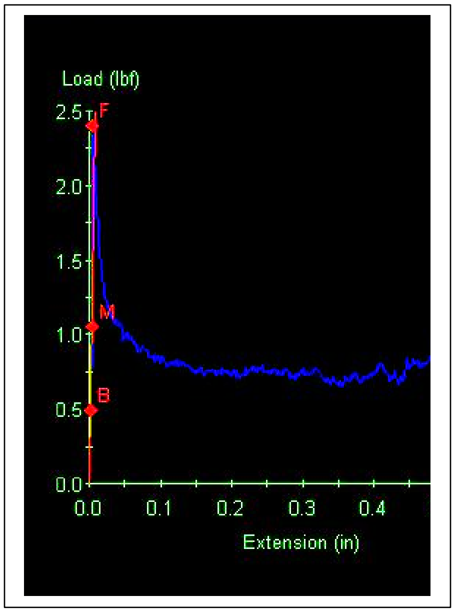

(a)

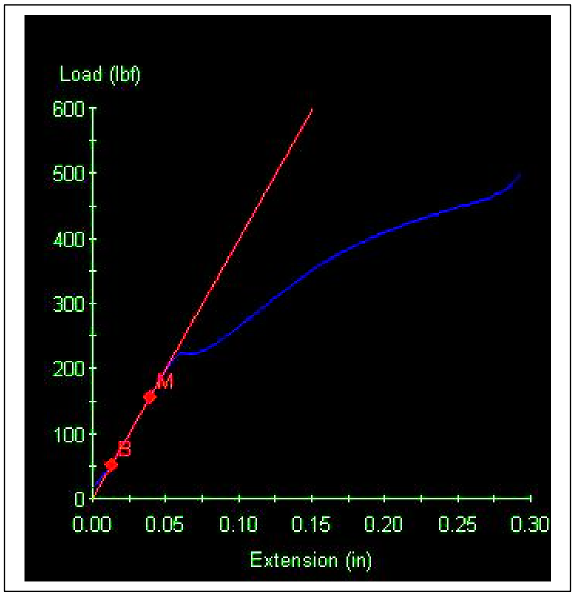

(b)

Figure 5.4.6: Pull out plots for the smooth surface rod (a) 1st ; (b) 2nd second pull-out

The experiments confirm the expected trends, with better overall retention of the coating in the rough surface specimen.

5.5 Preliminary In-Plant Evaluation

Production experiments with thin-wall die castings were conducted at General Die Casters in Peninsula. In preparation for these experiments, a spraying gun with a nozzle designed for spraying Boron Nitride was purchased. This nozzle has been evaluated and did not clog when used with BN.

An initial dilution ration of 2:1 was used for the initial experiments, with higher dilution ratios to be possibly evaluated later on.

Figure 5.5.1: Spray gun for BN

The production experiments with thin-wall die castings took place at General Die Casters in Peninsula. The ZYP BN coating was provided, along with a spraying gun. The casting was a thin-wall, large GE lamp head, about 20” long x 10” wide. Only a few shots were made. The operator stated he heard a “pop” during ejection of the part, and interpreted it as difficult ejection. He noted the sprayed coating deposited a hard shell, that spalled easily from the surface of the die. Following are pictures taken by GDC (Figures 5.5.2, 5.5.3).

Figures 5.5.2 and 5.5.3: Lamp die used for making thin wall lamp head castings

Further experiments are planned, possibly on a smaller casting, to gain more experience with the BN die lubricant.

6. Squeeze Casting of High Strength Aluminum Alloys

Squeeze casting of high strength aluminum alloys such as 201 and 206 can be challenging because of the well-known tendency of these alloys to hot tear. Experiments were conducted to determine the best parameters for squeeze casting these alloys. The experimental work was conducted on the 350 ton UBE squeeze caster at Case Western Reserve University shown in Figure 6.1. Plates of the size and shape shown in Figure 7.2 and Figure 7.3 were squeeze cast.

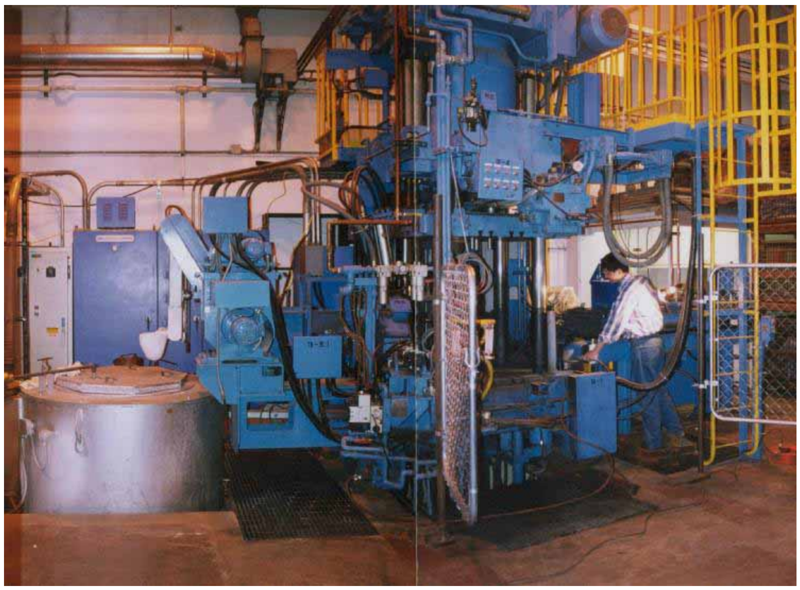

Figure 6.1: 350 ton Ube squeeze caster at Case Western Reserve University

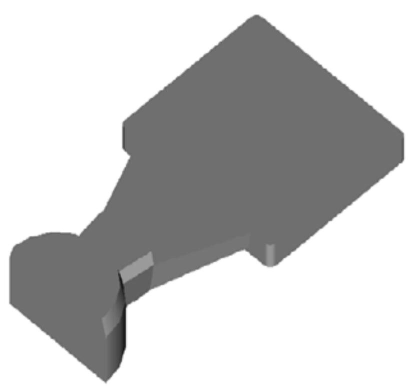

Cross-section of Ingate (in^2)	1.31
Ingate Shape	fanned
Volume of Casting (in^3)	13.73

Figure 6.2: Squeeze cast plate solid model

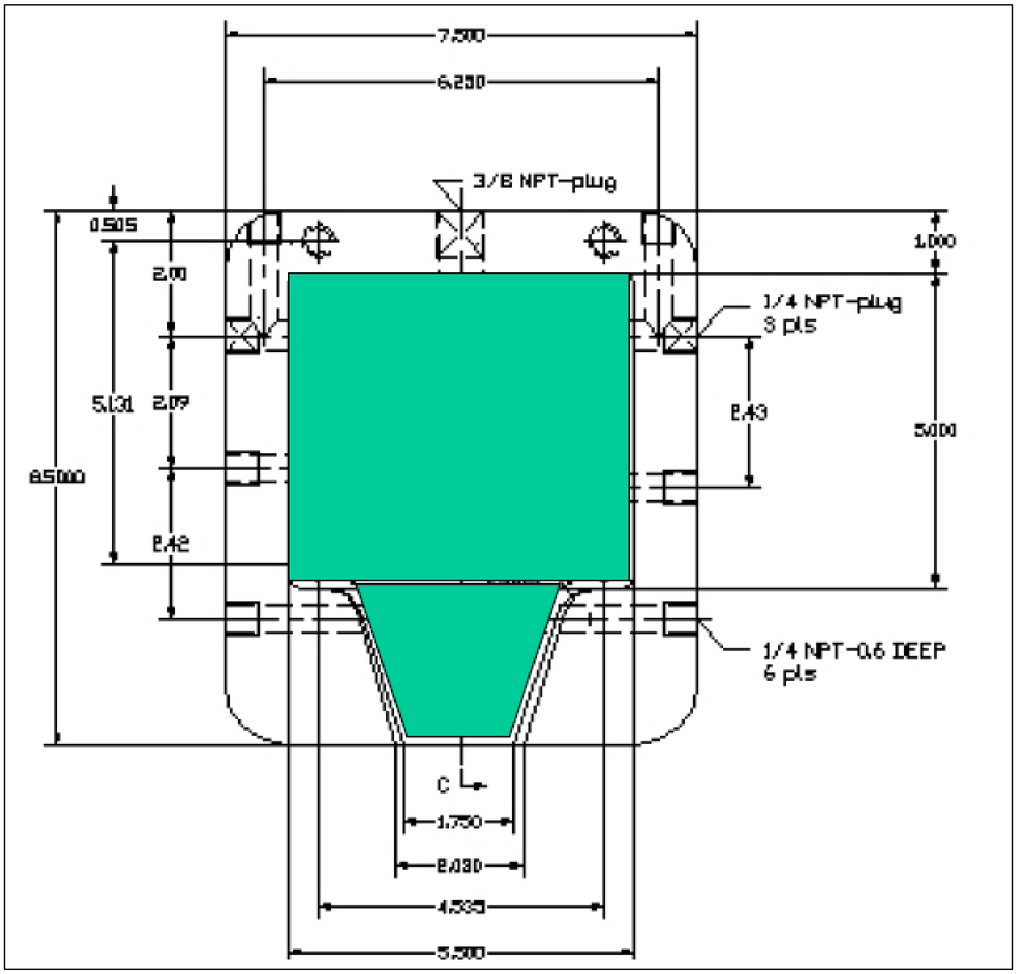

Figure 6.3: Squeeze cast plate dimensions

A fair quantity of 206 alloy was procured for the project. This alloy is known to pose hot tearing issues when casting complex shapes in metallic permanent molds or die casting dies. Squeeze casting experiments were carried out in a rectangular 5” x 5.5” x 0.5” insert as illustrated in Figures 6.2 and 6.3. Some of the plates showed evidence of hot tearing. Additional plates were cast in the 1,350-1,250 degrees F range to determine the effect of metal temperature on hot tearing. The as-squeezed cast plates are shown in Figure 6.4 still attached to the bisquit and in-gate.

Figure 6.4: As squeezed cast 204 plates

The tensile properties of the plates are shown in Figures 6.5 and 6.6. Both as-cast and T6 conditions were tested and are shown. Typical properties are tabulated in Table 6.1.

The noticeable scatter in properties originates from fine hot tearing cracks.

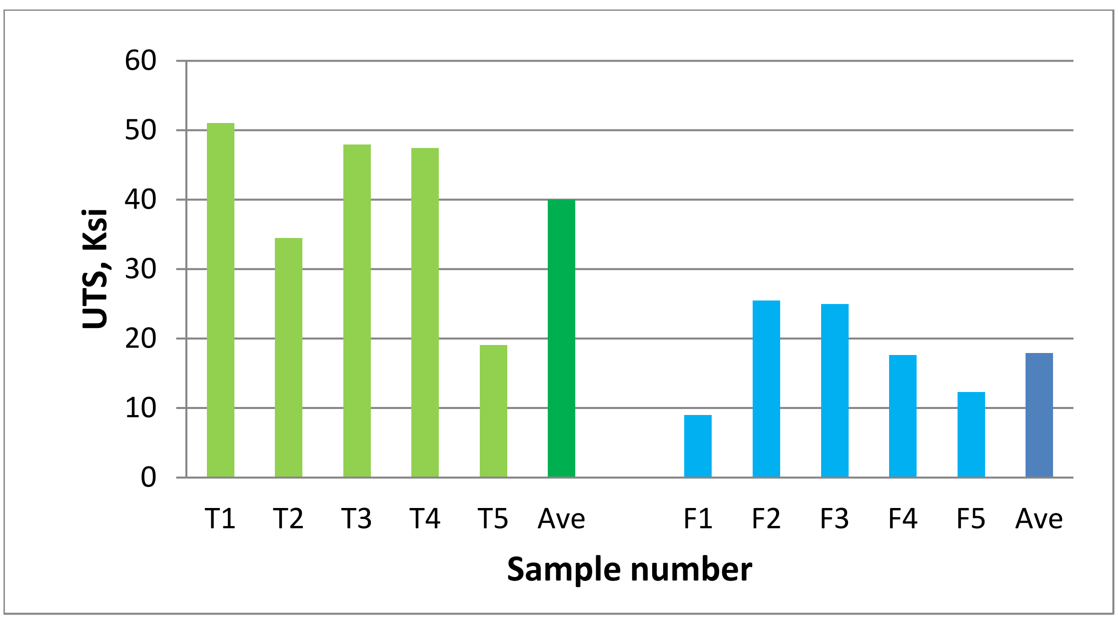

Figure 6.5: UTS of 206 squeeze cast plates in the as-cast (F) and heat treated (T6) state

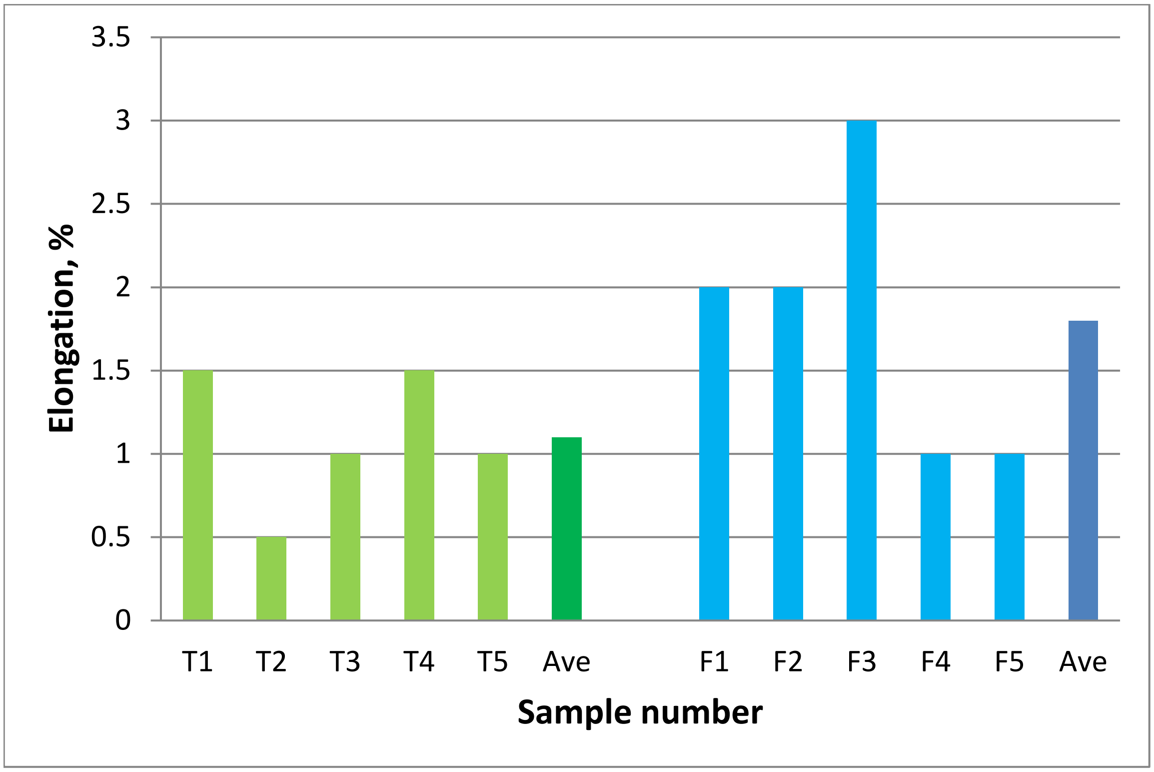

Figure 6.6: Elongation of 206 squeeze cast plate in as-cast (F) and heat treated (T6) condition

Table 6.1: Typical properties of 206 alloy

Properties		Conditions	
		T (°C)	Treatment
Density (×1000 kg/m^3)	2.6-2.8	25	
Poisson's Ratio	0.33	25	
Elastic Modulus (GPa)	70-80	25	
Tensile Strength (Mpa)	435	25	T7 (sand casting)
Yield Strength (Mpa)	345		
Elongation (%)	11.7		
Reduction in Area (%)			

The hot tearing trend of the alloy was investigated with the Constrained Rod Casting (CRC) for Hot Tearing Evaluation shown in Figure 7.6. The hot tearing tendency of the 206 alloy varies with processing conditions and is plotted in Figure 7.7 as a function of superheat.

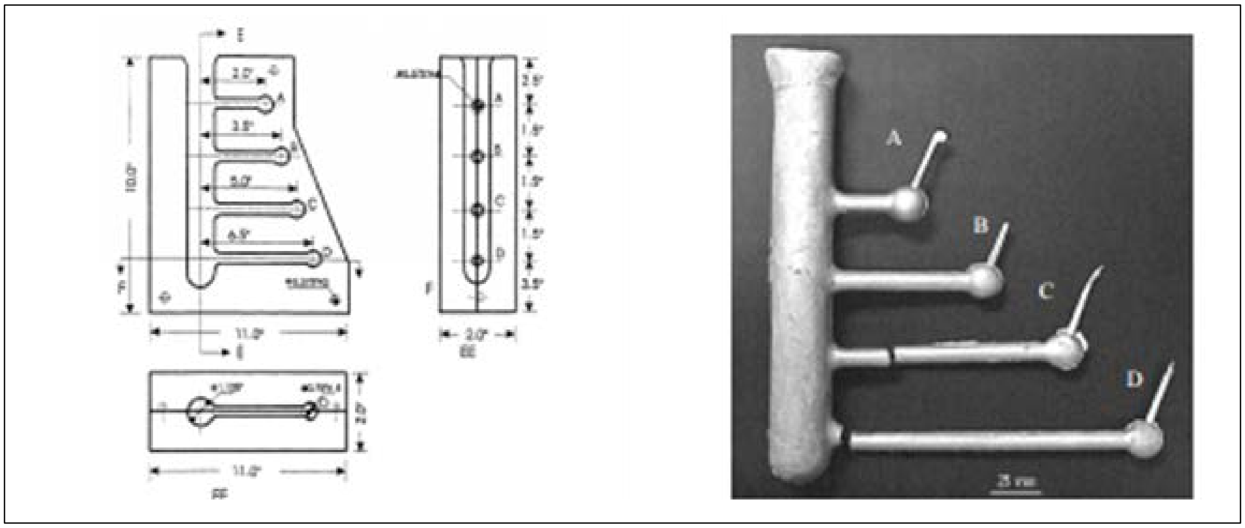

Figure 6.6: Constrained Rod Casting (CRC) for Hot Tearing Evaluation

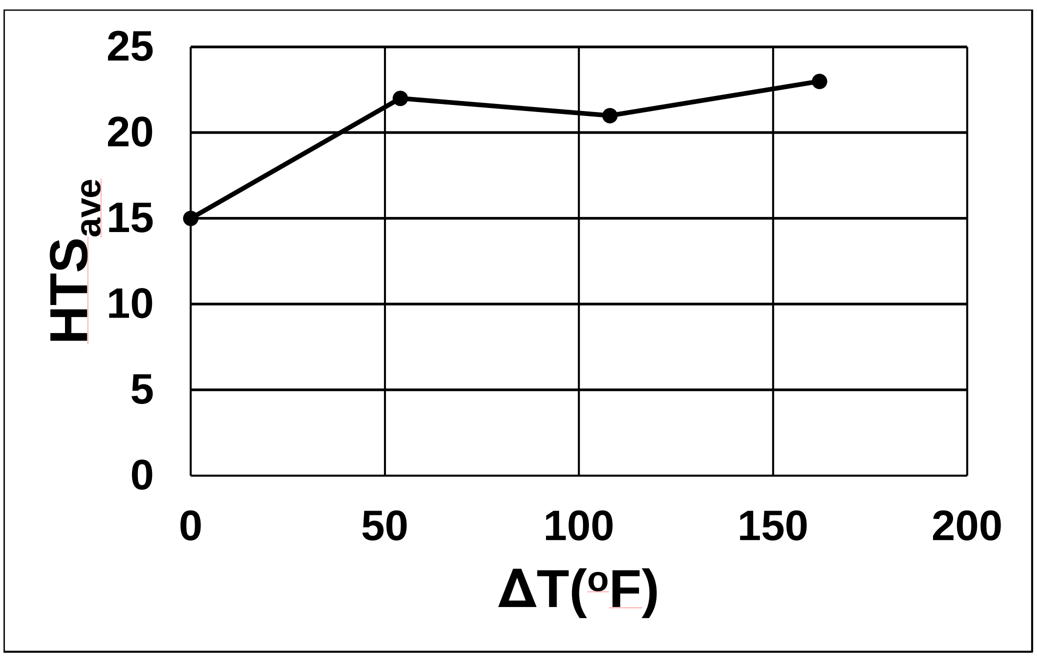

Figure 6.7: Hot tearing tendency of the 206 alloy as a function of superheat.

7. Conclusions

The initial focus of the project was to measure the fluidity of die casting aluminum alloys and increase it by changes in chemistry. To this end, a vacuum-based fluidity measurement system was designed and fabricated. The fluidity of mainstream commercial die casting aluminum alloys was measured with this setup. The high silicon 390 alloys was confirmed to provide the highest fluidity among these alloys. Attempts to further improve the fluidity of 390 with silicon and copper additions led to minor increases.

Parallel to the experimental work, a computational effort to predict influences of processing variables on fluidity was undertaken by Ohio State University. A relatively simple one-dimensional heat transfer model that incorporates part wall thickness, injection and die temperatures, gate speed plus the freezing range and fraction solid curve of the alloy was developed. The basic fluidity model was extended to incorporate varying speed and/or wall thickness. This extension enables analysis of prefill, or the situation where the cavity is partially filled before the onset of the fast shot or high-speed phase of cavity filling, and provides insight into the conditions under which prefill is beneficial and where it is not likely to be successful.

Several computation factorial experiments were performed using the basic model and analyzed to understand the relative importance of each factor as a contributor to flow distance. The results show that, while the alloy properties do affect the flow distance, flow distance or fluidity is largely a thermal issue controlled by the process conditions. This result provides support for the observation that the casting alloy should be selected to meet the functional requirements of the part without undue consideration of fluidity. The process conditions can then be optimized to produce an acceptable casting.

The computational work showed the injection velocity to be by far the most important variable in improving filling. The interfacial heat transfer between the die and the solidifying metal was also shown to have a significant impact on flow distance. This is an important takeaway, since it could be used by die casters to facilitate casting of thin-wall parts. For instance, lower thermal conductivity die materials or coatings could be used in thin sections to ensure filling. Implementation and evaluation of these methods are still underway at participating die casting collaborators.

Acknowledgments

The funding provided for this project by the Defense Logistics Agency and the management of Mr. Thornton White of Advanced Technology International are gratefully acknowledged. The technical input and coordination of the North American Die Casting Associations, its committees, and Mr. Stephen Udvardy, NADCA President, are also acknowledged. We are also grateful for the in-kind support received from General Die Casters, Momentive, Mercury Marine, and Badger Metal Tech.

References

Jorstad J.J. High Vacuum Die Casting NADCA Congress Proceedings, Paper T08-031, Atlanta GA, May 17-20, 2008.

Brown Z. High Vacuum Die Casting NADCA Congress Proceedings, Success story, Atlanta GA, May 17-20, 2008.

Herman E. Process and Die Engineering of Thin Wall Aluminum Die Castings, Die Casting Engineer, Sep. 2006, p.36.

Brown Z. Advancements in High Pressure Die Casting, NADCA Congress Proceedings, Paper T06-021, April 16-21, 2006, Columbus OH.

Emmenegger, J.Vacuum Die Casting Technology for Automotive Components, Paper T06-062, April 16-21, 2006, Columbus OH.

Robins, P. Vacuum-Assisted Die Casting Today’s Most Significant Technology, Paper T03-044, Indianapolis, IN

Pucher, P, Antrekowitsch, H. Bottcher, Kaufmann H, and Uggowitzer P.J. Influence of compositional variations on microstructural evolution, mechanical properties and fluidity of secondary foundry alloy AlSi9Cu3 Int. J. of Metals Research, Nov 2010, 375-383.

DiSabatino, M. Fluidity of Foundry Aluminum Alloys, PhD Thesis, Trondheim, September 2005, IMT-Report 2005:76